

ISTANBUL TECHNICAL UNIVERSITY ★ GRADUATE SCHOOL OF SCIENCE
ENGINEERING AND TECHNOLOGY

**IN SITU PREPARATION OF CYCLOHEXANONE FORMALDEHYDE
RESIN / LAYERED SILICATE NANOCOMPOSITES**

M.Sc. THESIS

Mehmet MERMUTLU

Department of Nano Science & Engineering

Nano Science & Engineering Programme

JANUARY 2013

ISTANBUL TECHNICAL UNIVERSITY ★ GRADUATE SCHOOL OF SCIENCE
ENGINEERING AND TECHNOLOGY

**IN SITU PREPARATION OF CYCLOHEXANONE FORMALDEHYDE
RESIN / LAYERED SILICATE NANOCOMPOSITES**

M.Sc. THESIS

**Mehmet MERMUTLU
(513101022)**

Department of Nano Science & Engineering

Nano Science & Engineering Programme

Thesis Advisor: Prof. Dr. Nilgün KIZILCAN

JANUARY 2013

İSTANBUL TEKNİK ÜNİVERSİTESİ ★ FEN BİLİMLERİ ENSTİTÜSÜ

**SİKLOHEKZANON FORMALDEHİT REÇİNE / KİL
NANOKOMPOZİTLERİNİN IN SITU HAZIRLANMASI**

YÜKSEK LİSANS TEZİ

**Mehmet MERMUTLU
(513101022)**

Nano Bilim & Mühendislik Anabilim Dalı

Nano Bilim & Mühendislik Programı

Tez Danışmanı: Prof. Dr. Nilgün KIZILCAN

OCAK 2013

Mehmet Mermutlu, a **M.Sc.** student of **Graduate School Of Science Engineering and Technology** student ID **513101022**, successfully defended the **thesis** entitled **“IN SITU PREPARATION OF CYCLOHEXANONE FORMALDEHYDE RESIN / LAYERED SILICATE NANOCOMPOSITES”**, which he prepared after fulfilling the requirements specified in the associated legislations, before the jury whose signatures are below.

Thesis Advisor : **Prof. Dr. Nilgün KIZILCAN**

Istanbul Technical University

Jury Members : **Asst. Prof. Dr. Birgül BENLİ**

Istanbul Technical University

Prof. Dr. Ayfer SARAÇ

Yıldız Technical University

Date of Submission : 13 December 2012
Date of Defense : 21 January 2013

FOREWORD

I would like to thank to my advisor, Prof. Dr. Nilgün KIZILCAN for her guidance, knowledge, encouragement, understanding and support throughout this project. She showed no hesitance to helping my problems during this work. Also, I would like to thank to my parents, for their patience, understanding and support during all stages of my education.

December 2012

Mehmet MERMUTLU
(Chemist)

TABLE OF CONTENTS

	<u>Page</u>
FOREWORD	vii
TABLE OF CONTENTS	ix
ABBREVIATIONS	xi
LIST OF TABLES	xiii
LIST OF FIGURES	xv
SUMMARY	xvii
ÖZET	xix
1. INTRODUCTION	1
2. THEORETICAL PART	3
2.1. Composites	3
2.1.1. Polymer matrix materials	4
2.2. Resins	5
2.2.1. Thermoset resins	5
2.2.2. Thermoplastic resins	6
2.2.3. Advantages and disadvantages of thermoplastic resins	7
2.2.4. Ketone and aldehyde resins	8
2.2.4.1. Aliphatic and cycloaliphatic ketone resins	9
2.2.4.2. Methyl ethyl ketone formaldehyde resins	10
2.2.4.3. Acetone formaldehyde resins	11
2.2.4.4. Cyclohexanone resins	11
2.2.4.5. Cyclohexanone formaldehyde resins	12
2.3. Nanocomposites	13
2.3.1. Polymer / clay nanocomposites	15
2.3.2. Resin / clay nanocomposites	16
2.3.2.1. Epoxy resin nanocomposites	16
2.3.2.2. Phenolic resin nanocomposites	17
2.3.2.3. Urea formaldehyde resin nanocomposites	17
2.3.3. Nanocomposite preparation	18
2.3.4. Nanoparticle dispersion in polymers	19
2.3.5. Montmorillonite	20
2.2.6. Agglomeration of nanoparticles in polymer matrix	21
3. EXPERIMENTAL PART	23
3.1. Materials	23
3.2. Synthesis of Cyclohexanone Formaldehyde Resin (CFR)	23
3.3. Synthesis of DA.PDMS Modified Cyclohexanone Formaldehyde Resin (DA.PDMS-CFR)	23
3.4. Synthesis of Layered Clay Nanocomposites of Cyclohexanone Formaldehyde Resin Samples (LC-CFR)	24
3.5. Synthesis of DA.PDMS Modified Layered Clay Nanocomposites of Cyclohexanone Formaldehyde Resin (DA.PDMS-LC-CFR)	24
3.6. Characterization of CFR, DA.PDMS-CFR, LC-CFR and DAPDMS-LC-CFR Samples	25

4. RESULT AND DISCUSSION	27
4.1. Reaction Mechanism and Characterization of CFR.....	27
4.1.1. ¹ H-NMR spectroscopy of CFR	28
4.1.2. FTIR-ATR spectroscopy of CFR.....	28
4.1.3. DSC thermal analysis of CFR.....	29
4.2. Reaction Mechanism and Characterization of DA.PDMS-CFR	30
4.2.1. ¹ H-NMR spectroscopy of DA.PDMS-CFR.....	31
4.2.2. FTIR-ATR spectroscopy of DA.PDMS-CFR.....	32
4.2.3. DSC thermal analysis of DA.PDMS-CFR	33
4.3. Characterization of MMT Clay.....	34
4.3.1. FTIR-ATR spectroscopy of MMT clay.....	34
4.3.2. XRD analysis of MMT clay	35
4.4. Characterization of LC-CFR Nanocomposite Samples	35
4.4.1. FTIR-ATR spectroscopy of LC-CFR nanocomposite samples	35
4.4.2. DSC thermal analysis of LC-CFR samples	37
4.4.3. TGA thermal analysis of LC-CFR samples.....	38
4.4.4. XRD analysis of LC-CFR samples	40
4.4.5. SEM analysis of LC-CFR samples	41
4.5. Characterization of DA.PDMS-LC-CFR Nanocomposite Samples	43
4.5.1. FTIR-ATR spectroscopy of LC-CFR nanocomposite samples	43
4.5.2. DSC thermal analysis of DA.PDMS-LC-CFR samples.....	45
4.5.3. TGA thermal analysis of DA.PDMS-LC-CFR samples	46
4.5.4. XRD analysis of DA.PDMS-LC-CFR samples	48
4.5.5. SEM analysis of DA.PDMS-LC-CFR samples	49
5. CONCLUSION	51
REFERENCES	53
CURRICULUM VITAE	59

ABBREVIATIONS

CF	: Cyclohexanone Formaldehyde
CFR	: Cyclohexanone Formaldehyde Resin
DA.PDMS	: Diamine Terminated Polydimethylsiloxane
DA.PDMS-CFR	: DA.PDMS modified Cyclohexanone Formaldehyde Resin
DA.PDMS-LC-CFR	: DA.PDMS-CFR / Layered Clay Nanocomposite
DSC	: Differential Scanning Calorimetry
FTIR-ATR	: Fourier Transform Infrared- Attenuated Total Reflectance
LC-CFR	: CFR / Layered Clay Nanocomposite
MMT	: Montmorillonite Clay
NMR	: Nuclear Magnetic Resonance Spectroscopy
SEM	: Scanning Electron Microscope
T_g	: Glass Transition Temperature
TGA	: Thermogravimetric Analysis
XRD	: X-ray Diffraction Spectroscopy

LIST OF TABLES

	<u>Page</u>
Table 3.1: Contents of LC-CRF nanocomposite samples	24
Table 3.2: Contents of DA.PDMS-LC-CRF nanocomposite samples	25
Table 4.1: Characteristic literature wavenumber values and observed wavenumber values of of CFR	29
Table 4.2: Characteristic literature wavenumber values of DA.PDMS-CFR and observed wavenumber values of DA.PDMS-CFR	33
Table 4.3: TGA values of CFR and LC-CFRs	39
Table 4.4: Interlayer spaces between clay sheets of LC-CFR samples	41
Table 4.5: TGA values of DA.PDMS-CFR and DA.PDMS-LC-CFRs	47
Table 4.6: Interlayer spaces between clay sheets of DA.PDMS-LC-CFR samples ..	49

LIST OF FIGURES

	<u>Page</u>
Figure 2.1: Classification of matrices in composite materials	4
Figure 2.2: Monomers using in resin synthesis	9
Figure 2.3: Dispersion of nanoparticles in polymers	19
Figure 2.4: Montmorilloite structure T: Tetrahedral sheet; O: Octahedral sheet	21
Figure 4.1: Reaction mechanism of CFR	27
Figure 4.2: ¹ H-NMR spectrum of CFR	28
Figure 4.3: FTIR spectrum of CFR	29
Figure 4.4: DSC thrmogram of CFR.	30
Figure 4.5: Reaction mechanism of DA.PDMS-CFR	31
Figure 4.6: ¹ H-NMR spectrum of DA.PDMS-CFR	32
Figure 4.7: FTIR spectrum of DA.PDMS-CFR	32
Figure 4.8: DSC thrmogram of DA.PDMS-CFR	34
Figure 4.9: FTIR spectrum of MMT clay	34
Figure 4.10: XRD pattern of MMT clay	35
Figure 4.11: FTIR spectrum of LC-CFR1	36
Figure 4.12: FTIR spectrum of LC-CFR2	36
Figure 4.13: FTIR spectrum of LC-CFR3	37
Figure 4.14: FTIR spectrum of LC-CFR4	37
Figure 4.15: Variation of Tg (oC) for various resin clay nanocomposites with different filler contents	38
Figure 4.16: DSC thermogram of LC-CFR samples.	38
Figure 4.17: TGA thermograms of CFR and LC-CFRs	39
Figure 4.18: XRD patterns of LC-CFR samples	40
Figure 4.19: SEM images of LC-CFR1 (a; x15,000, b; x80,000)	41
Figure 4.20: SEM images of LC-CFR2 (a; x15,000, b; x50,000)	42
Figure 4.21: SEM images of LC-CFR3 (a; x15,000, b; x50,000)	42
Figure 4.22: SEM images of LC-CFR4 (a; x15,000, b; x15,000).	42
Figure 4.23: FTIR spectrum of DA.PDMS-LC-CFR1	43
Figure 4.24: FTIR spectrum of DA.PDMS-LC-CFR2	44
Figure 4.25: FTIR spectrum of DA.PDMS-LC-CFR3	44
Figure 4.26: FTIR spectrum of DA.PDMS-LC-CFR4	45
Figure 4.27: Variation of Tg (oC) for various resin clay nanocomposites with different filler contents.	45
Figure 4.28: DSC thermogram of LC-CFR samples	46
Figure 4.29: TGA thermograms of DA.PDMS-CFR and DA.PDMS-LC-CFRs	47
Figure 4.30: XRD patterns of LC-CFR samples	48
Figure 4.31: SEM images of DA.PDMS-LC-CFR1 (a; x7,500, b; x50,000)	49
Figure 4.32: SEM images of DA.PDMS-LC-CFR2 (a; x15,000, b; x50,000)	50
Figure 4.33: SEM images of DA.PDMS-LC-CFR3 (a; x15,000, b; x50,000)	50
Figure 4.34: SEM images of DA.PDMS-LC-CFR3 (a; x15,000, b; x50,000)	50

IN SITU PREPARATION OF CYCLOHEXANONE FORMALDEHYDE RESIN / LAYERED SILICATE NANOCOMPOSITES

SUMMARY

Polymer / layered silicate nanocomposites show enhanced properties, opposed to the high volume fraction loading (>50%) in traditional advanced composites, at very low volume fraction loading (1-5%) of layered silicates. Commercial resins are generally solid materials with low molecular weight and they can be processed easily. They are often mixed with cellulose nitrate and alkyd resins for coating applications. This type of resins are mainly used in surface coatings, varnishes, inks, textile and paper industries as additive materials. Previous studies demonstrated the synthesis of copolymers of CF resins is possible with polydimethylsiloxanes (PDMS) by one step method of in situ modification of ketonic resin.

In this study, in situ modified cyclohexanone formaldehyde resin samples and nanocomposite forms of these resins were prepared from direct addition of MMT clay (montmorillonite: whose cation-exchange capacity is 80 meq / 100 g sodium, average particle sizes are smaller than 10 μm , density is 2,6 g cm^3) and amine chain ended polydimethylsiloxane (bis(3-aminopropyl) terminated), DA.PDMS, in the presence of base catalyst. Different clay contents (from 0,5 to 3 wt%) were used to produce clay modified nanocomposite resins. With this method PDMS modified polymeric nanocomposite material would be synthesized in one step.

The characterizations of the final samples were performed by fourier transform infrared spectroscopy (FTIR-ATR), nuclear magnetic resonance spectroscopy (NMR), differential scanning calorimetry (DSC), X-ray diffractometer (XRD) and scanning electron microscopy (SEM). In FTIR-ATR measurements, with the characteristic peaks of neat cyclohexanone formaldehyde resin, Si-O-Si stretch and Si-CH₃ peaks of PDMS and O-H stretching of structural OH groups and Si-O deformation peaks of clay were obtained for nanocomposite resin copolymer samples. Methylol bridges, N-H and Si-CH₃ bonds of resin copolymer samples observed with using ¹H-NMR spectroscopy. The effect of the clay amount on the thermal properties of materials were investigated by DSC. Glass transition temperatures (T_g) of resin and resin / clay nanocomposite samples were determined. Basal spacing between clay sheets in nanocomposites investigated and calculated by XRD. Distribution of clay particles in polymeric resin matrix and morphology of samples were determined with SEM.

SİKLOHEKZANON FORMALDEHİT REÇİNE / KİL NANOKOMPOZİTLERİNİN IN SITU HAZIRLANMASI

ÖZET

Nanokompozitler, seçilen bir matris içerisinde nanometre boyutunda parçacıkların dağılması ile elde edilirler. Matris seçimi için polimer, seramik, metal gibi bir çok malzeme seçilebileceği gibi, matris içerisinde dağılan nanomalzeme de inorganik, organik, kristal veya yarı kristal olabilir. Kullanılan nano malzemelerin boyutları bir boyutlu da olabilir iki veya üç boyutlu da olabilir. Örnek olarak, bu çalışma sırasında kullanılan montmorilonit kili tabakalı bir yapıya sahip olup, iki oyutlu bir malzemedir. Her bir tabakasının kalınlığı 1-2 nm civarında, uzunluğu ise 100-200 nm civarındadır.

Nano malzemelerin matris içerisinde dağılımlarını etkili bir şekilde yapmak için doğru sentez tekniği seçilmelidir. Çeşitli bir çok sentez tekniğinden bahsedilebilir. Kompozit malzemeler, in situ interkalatif polimerizasyon, eriyik maddenin katkı maddesi ile karıştırılması ve başka bir çok yöntemle hazırlanabilir. Bu iki teknik birçok araştırmacı tarafından en çok kullanılan nanokompozit hazırlama teknikleridir. Özellikler bu çalışmadaki gibi polimer / kil kompozit malzemeleri hazırlamak için en çok in situ polimerizasyon tercih edilmektedir. Polimer malzemenin kendi elde edilme reaksiyonu gerçekleşirken içerisine eklenen kilin homojen dağıtılması ve tabakalar arası mesafenin aralanması sağlanmış olur.

Polimer / kil nanokompozitlerin, klasik kompozitlerdeki katkı oranına (>50%) karşın, çok düşük miktarda tabakalı silikat (1-5%) eklenmesiyle bile, birçok özelliklerinde gelişmişlik gözlenir. Klasik kompozitlerin göstermiş olduğu özelliklerin gelişmişliği çok uzun zamandır bilinmektedir ve bu gelişmişlikler nanokompozitler ile daha da arttırılmıştır. Nano kompozitlerin gösterdiği çeşitli özellikler klasik kompozitlere kıyasla çok daha fazladır. Bunlar mekanik, termal, optik, elektriksel iletkenlik gibi birçok yönde olabilir. Bunun en temel nedeni katkı maddesi olarak kullanılan nano malzemelerdeki yüzey alanının hacme olan oranının klasik kompozitlerdeki katkı malzemelerine oranla çok daha fazla olmasıdır. Bunun doğal sonucu olarak katkı maddesi ve matris arasındaki etkileşim çok daha fazla olur.

Polimer matris olarak poliimidler, poliamidler, çeşitli reçineler ile yapılan bir çok çalışma mevcuttur. Bu çalışmada polimer malzeme olarak bir ketonik reçine olan siklohekzanon formaldehit reçinesi kullanıldı. İçerisinde dağıtılan nano malzeme olarak ise bir tabakalı kil olan montmorilonit kullanıldı. Kullanılan kilin en önemli özelliği düşük maliyetine rağmen malzemeye vermiş olduğu gelişmişlik derecesidir. Tabakalı killer montmorillonit, betonit gibi bir çok madde olabilir. Killer bir çok organik zincir molekülleri ile modifiye edilebilirler, bunun neticesinde matris içerisinde dağılmaları, kil moleküllerinin matris ile etkileşmelerinin artmasından dolayı daha da kolaylaşır.

Tabakalı killerin matris içerisinde dağılımı da önemli bir konudur. Nano parçaların, killer gibi, aralarındaki etkileşimlerle bir araya gelme eğilimleri vardır ve bu nedenle yüksek katılım oranlarında homojen kompozit malzeme elde etmek zordur. Tabakalı killerin matris içerisinde dağılımı kil tabakalarının arasındaki mesafenin aralanması ile değerlendirilir. Mesafenin doğru polimer seçimi ve değişik yöntemlerle, kil modifiye etmek gibi, daha fazla artırılması mümkündür. Tabakaların aralanması ile polimer ile kil tabakalarının etkileşimi daha fazla olacağından özelliklerindeki gelişmişlikler giderek artar. Bu aralanma genel olarak üç guruba ayrılabilir. Bunlar, kasık kompozit yapıdaki gibi tabakaların çok çok az aralanması, bir diğeri tabakalar arası mesafenin ciddi derecede aralanması ve matrisin bu aralanan tabakalar arasına yerleşmesi, sonuncusu ise kil tabakalarının birbirlerinden bağımsız olarak yani tamamen ayrılarak matris içerisinde dağılması olarak tanımlanabilir. Son bahsedilen aralanma miktarına ulaşmak, gerek nano malzemelerin aralarında ki etkileşimlerden olsun gerekse yapılarının kararlılığından olsun, kolay değildir. Kil tabakalarının tam aralanması gerçekleşmese bile aralarında ki mesafenin olabildiğince arttırılmak istenmesi önemlidir. En iyi gelişmiş özellikler bu yapı da gözlemlenmektedir.

Kilin polimer içerisinde dağılışı sırasında gözlemlenebilecek bir diğeri önemli olay ise kil nano partiküllerinin bir araya gelerek topaklanma istekleridir. Bu partiküller arası etkileşim aslında zayıf iyonik kuvvetlerden ve zayıf Van der Waals etkileşimlerinden ileri gelmektedir. Bu etkileşimler zayıf olabilir fakat, partiküllerinin boyutlarının çok küçük olması ve yüzey alanlarının bu boyutta çok yüksek olması ile birlikte sayıca çok artmakta ve böylece aralarında kuvvetli bir etkileşime yol açmaktadır. Bu da kil nano partiküllerinin matris içerisinde bir yüzdeyi geçtikten sonra bir araya gelmelerine neden olmaktadır. Bu son derece istenmeyen bir durumdur, çünkü malzemenin özelliklerinde gerilemeye neden olmaktadır.

Polimer nano kompozit malzemelerin kullanım alanları olarak uçak, savunma, elektronik, ilaç, enerji gibi bir çok alan örnek olarak gösterilebilir. Bu alanlarda ve diğeri alanlarda polimer nano kompozitlerin kullanımı yapılan çalışmalar ve elde edilen bulgular ışığında her geçen gün artmakta ve daha fazla araştırmacının dikkatini çekmektedir. Bunun en temel nedeni, tabii ki, zaten kullanılmakta olan doğal malzemelerin bulunabilme zorlukları ve bunun hep devam etmesidir. İleride bu tip kompozit malzemeleri markette daha sık görmek mümkün olacaktır.

Ticari reçineler; genellikle katı, düşük molekül ağırlıklı ve kolay işlenebilir malzemelerdir. Genellikle selüloz nitrat ve alkid reçineler ile karıştırılarak yüzey kaplama uygulamalarında kullanılırlar. Bu reçinelerin en çok yüzey kaplama, vernik, mürekkep, tekstil ve kağıt endüstrisinde katkı maddesi olarak kullanılırlar. Önceki çalışmalar, ketonik reçinelerin, tek aşamalı in situ modifikasyon ile, polidimetilsiloksanlarla kopolimer oluşturabileceğini göstermektedir. Bu çalışmada hem modifiye edilmiş hem de edilmemiş reçine içerisinde ham kilin dağılımı incelendi.

Bu çalışmada, in situ modifikasyon ile elde edilen sikloheksanon formaldehit reçine örnekleri ve bunların nanokompozit formları MMT kilinin (kasyon değiştirme kapasitesi 80 meq / 100 g olan, ortalama tanecik boyutu 10 µm ve yoğunluğu 2,6 g cm³ olan montmorillonite) ve amin sonlu polidimetilsiloksanın (bis(3-adminopropyl) in situ reaksiyon ortamına bazik ortamda direk reaksiyon ortamına eklenmesi ile elde edildi. Kütlece %0.5 ten %3' e kadar değişik kil oranları denendi. Bu yöntemle

polidimetilsiloksan modifiyeli polimer / kil nanokompozitleri bir aşamada sentezlenmiş oldu.

Elde edilen örneklerin karakterizasyonu bir çok spektroskopik, termal vb. yöntem kullanılarak yapıldı. Kimyasal yapının tayin edilmesi için fourier dönüşümlü infrared spektroskopisi (FTIR-ATR) ve nükleer manyetik rezonans spektroskopisi (NMR), kullanıldı. Sentezlenen örneklerin termal özelliklerinin belirlenmesi için kademeli tarayıcı kalorimetri (DSC) ve termal gravimetrik analiz (TGA) yöntemleri kullanıldı. Morfolojinin daha iyi anlaşılması için sentezlenen örnekler X ışınları kırınımı (XRD) ve taramalı elektron mikroskopisi (SEM) ile incelendi.

FTIR-ATR sonuçları ile sikloheksanon formaldehit reçinesinin karakterisitk pikleri rahat bir şekilde gözlemlenebilir. Bunun yanında polidimetilsiloksan modifiyeli sikloheksanon formaldehit reçinesi için Si-O-Si ve Si-CH₃ gerilim pikleri sentezlenen örneklerde gözlemlendi. Sentezlenen nanokompozit örnekleri içerisindeki kil moleküllerinin Si-O deformasyon pikleri, bu örneklerdeki en belirgin ve ayırt edici pik olarak gözlemlendi.

Kimyasal yapının tayini için kullanılan bir diğer yöntem olan ¹H-NMR spektroskopisi ile sentezlenen örneklerdeki metilol köprüleri, N-H ve Si-CH₃ pikleri gözlemlendi.

Kilin reçine kopolimer örnekleri içerisindeki dağılımı ile meydana gelen termal davranışındaki değişimler DSC ve TGA ile incelendi. Nanokompozitlerdeki camı geçiş sıcakları (T_g), bozunmanın başlama sıcaklığı ve belirli değerlerdeki kalıntı miktarları belirlendi. Bu verilerden yola çıkılarak sentezlenen reçine malzemelerinin nanokompozit formlarının saf hallerine göre termal olarak daha dayanıklı oldukları gözlemlendi.

Nanokompozitlerdeki kil tabakaları ve tabakaların basal boşluk mesafeleri XRD ile incelendi. Bu veriler ışığında kilin tabakalar arası boşluklarının artmış olduğu ve yapının istenildiği gibi gerçekleştiği kanıtlandı. Kilin polimerik reçine içerisindeki homojen dağılımı ve örneklerin morfolojileri SEM ile incelendi. Sentezlenen nonaokompozit numunelerindeki kil oranının kütlece %3 olduğu durumlar için kil nanoparçacıklarının topaklanması gözlemlendi.

1. INTRODUCTION

Blended organic and inorganic components called hybrid materials, either occurring naturally or prepared synthetically, have gained much interest in industry and research communities [1-7]. Polymers are commonly used materials and over periods of time their applications have increased in our lives. Therefore, it is necessary to develop new polymeric materials with improved properties to address the growing number of applications. The maximum benefits of nanoscience can be defined by developing materials providing multiple advantageous properties and designing such materials by incorporating various properties is therefore vital. Polymer nanocomposite materials are a particular kind of synthetic hybrid material, which shows multiple unique properties [8-18]. To enhance the properties of a polymer, fillers are often added to obtain a homogeneous mixture called a composite. If one of the dimensions of the filler particles is in the nanometer range then these composite materials are termed as polymer nanocomposites. The transition of length scale from micrometer to nanometer yields dramatic changes in physical properties as nano scale particles have a large surface area for a given volume. Usually fillers used are inorganic in nature, and act as reinforcing material. The role of the matrix is to adhere and to bind fillers. The resulting material will have properties which will be a combination of the individual properties of polymer and filler particles. The properties of polymer nanocomposites depend not only on the properties of individual components but also on their morphology and interfacial interactions [19]. The effective properties of polymer nanocomposites are dependent on various filler properties, such as their size, area, aggregate structure, surface chemistry, and interactions with the polymer matrix, all of which will affect the dispersion of inorganic fillers in the polymer matrix. Due to its extreme utility and importance both in research and industry, it becomes imperative to understand the relationship between the microstructure and the macroscopic properties that are of interest. To achieve maximum property enhancement a homogeneous dispersion of nanoscale fillers is highly desired [20-21].

As a result there is a need to understand the design of nanometer scale architecture and factors affecting such structures and how they can affect the final properties of materials. Often these improvements in properties may occur at the expense of other useful polymeric properties, such as thermal behaviors, mechanical toughness and crack resistance. Consequently it is highly desirable to be able to use fillers which can improve properties, but not at the cost of polymeric properties.

It can be said that the smaller the diameter, the greater the surface area per unit volume. Particle diameter changing, layer thickness, or fibrous material diameter from the micrometer to the nanometer range will affect the surface area-to-volume ratio thereby affecting surface interactions and thus final properties [22-26].

As a nanoscale material, layered silicate montmorillonite clay was used to obtain nanocomposites forms of in situ modified with polydimethylsiloxane cyclohexanone formaldehyde resins in this study. Also, samples were studied with using several characterization techniques.

2. THEORETICAL PART

2.1. Composites

The term composite could mean almost anything if taken at face value, since all materials are composed of dissimilar subunits if examined at close enough detail. But in modern materials engineering, the term usually refers to a matrix material that is reinforced with fibers. For instance, the term FRP (for Fiber Reinforced Plastic) usually indicates a thermosetting polyester matrix containing glass fibers, and this particular composite has the lion's share of today's commercial market [27].

Composites that forms heterogeneous structures which meet the requirements of specific design and function, imbued with desired properties which limit the scope for classification. However, this lapse is made up for, by the fact new types of composites are being innovated all the time, each with their own specific purpose like the filled, flake, particulate and laminar composites. Fibers or particles embedded in matrix of another material would be the best example of modernday composite materials, which are mostly structural.

Composites cannot be made from constituents with divergent linear expansion characteristics. The interface is the area of contact between the reinforcement and the matrix materials. In some cases, the region is a distinct added phase. Whenever there is interphase, there has to be two interphases between each side of the interphase and its adjoint constituent. Some composites provide interphases when surfaces dissimilar constituents interact with each other. Choice of fabrication method depends on matrix properties and the effect of matrix on properties of reinforcements. One of the prime considerations in the selection and fabrication of composites is that the constituents should be chemically inert non-reactive. Classification of matrices could be seen in Figure 2.1.

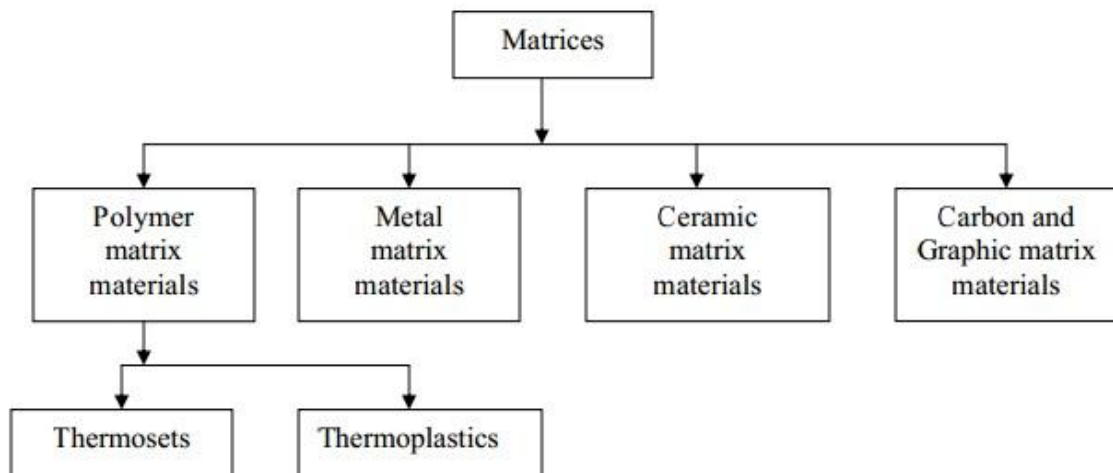


Figure 2.1: Classification of matrices in composite materials.

2.1.1. Polymer matrix materials

Polymers make ideal materials as they can be processed easily, possess lightweight, and desirable mechanical properties. It follows, therefore, that high temperature resins are extensively used in aeronautical applications.

Two main kinds of polymers are thermosets and thermoplastics. Thermosets have qualities such as a well-bonded three-dimensional molecular structure after curing. They decompose instead of melting on hardening. Merely changing the basic composition of the resin is enough to alter the conditions suitably for curing and determine its other characteristics. They can be retained in a partially cured condition too over prolonged periods of time, rendering Thermosets very flexible. Thus, they are most suited as matrix bases for advanced conditions fiber reinforced composites. Thermosets find wide ranging applications in the chopped fiber composites form particularly when a premixed or moulding compound with fibers of specific quality and aspect ratio happens to be starting material as in epoxy, polymer and phenolic polyamide resins. Thermoplastics have one or two dimensional molecular structure and they tend to at an elevated temperature and show exaggerated melting point. Another advantage is that the process of softening at elevated temperatures can be reversed to regain its properties during cooling, facilitating applications of conventional compress techniques to mould the compounds.

Resins reinforced with thermoplastics now comprised an emerging group of composites. The theme of most experiments in this area to improve the base

properties of the resins and extract the greatest functional advantages from them in new avenues, including attempts to replace metals in die-casting processes. In crystalline thermoplastics, the reinforcement affects the morphology to a considerable extent, prompting the reinforcement to empower nucleation. Whenever crystalline or amorphous, these resins possess the facility to alter their creep over an extensive range of temperature. But this range includes the point at which the usage of resins is constrained, and the reinforcement in such systems can increase the failure load as well as creep resistance [28].

2.2. Resins

Most of the commercial resins are generally solid materials with low molecular weight. Also they can be processed easily. These types of resins are mainly used in surface coatings, varnishes, inks, textile and paper industries as additive materials [29].

If we give a definition for resin, according to DIN 55947, resin is the general term used technically for solid, hard to soft, organic, noncrystalline products having a broader or narrower molecular mass distribution. They normally have a melting or softening range, are brittle in the solid state, and then usually show conchoidal (shell-like) fracture. They have a tendency to flow at room temperature (“cold flow”). Resins are in general raw materials, for example for binders, curable moulding compositions, adhesives and coatings.

There are another definitions for resins for example, European Standard CEN/TC 139, a resin is somewhat different and more concise: “A solid, semisolid or liquid substance of nonuniform and often high molecular weight, which in the solid state usually possesses a softening or melting range and exhibits conchoidal fracture”
Note: In the broader sense, this expression is used to denote any polymer which forms the basis of a thermoplastic. Following agreement, bitumen, grades of pitch, gums and waxes are excluded [30].

2.2.1. Thermoset resins

The most common thermosetting resin used today is polyester resin, followed by vinyl ester and epoxy. Thermosetting resins are popular because uncured, at room

temperature, they are in a liquid state. This allows for convenient impregnation of reinforcing fibers such as fiberglass, carbon fiber, or Kevlar.

A room temperature liquid resin is easy to work with. Laminators can easily remove all air during manufacturing, and it also allows the ability to rapidly manufacture products using a vacuum or positive pressure pump. (Closed Molds Manufacturing) Beyond ease of manufacturing, thermosetting resins can exhibit excellent properties at a low raw material cost.

Properties of thermoset resins includes; Excellent resistance to solvents and corrosives, Resistance to heat and high temperature, Fatigue strength, Tailored elasticity, Excellent adhesion, Excellent finishing (polishing, painting, etc.)

In a thermoset resin, the raw uncured resin molecules are crossed linked through a catalytic chemical reaction. Through this chemical reaction, most often exothermic, the resin creates extremely strong bonds to one another, and the resin changes state from a liquid to a solid.

A thermosetting resin, once catalyzed, it can not be reversed or reformed. Meaning, once a thermoset composite is formed, it cannot be remolded or reshaped. Because of this, the recycling of thermoset composites is extremely difficult. The thermoset resin itself is not recyclable, however, there are a few new companies who have successfully removed the resin through pyrolyzation and are able to reclaim the reinforcing fiber.

2.2.2. Thermoplastic resins

Thermoplastic polymer resins are extremely common, and we come in contact with thermoplastic resins constantly. Thermoplastic resins are most commonly unreinforced, meaning, the resin is formed into shapes and have no reinforcement providing strength.

Examples of common thermoplastic resins using today and their applications:

- PET - Water and soda bottles
- Polypropylene - Packaging containers
- Polycarbonate - Safety glass lenses
- PBT - Children's Toys
- Vinyl - Window frames

- Polyethylene - Grocery bags
- PVC - Piping
- PEI - Airplane armrests
- Nylon - Footwear

Many thermoplastic products use short discontinuous fibers as a reinforcement. Most commonly fiberglass, but carbon fiber too. This increases the mechanical properties and is technically considered a fiber reinforced composite, however, the strength is not nearly as comparable to continuous fiber reinforced composites.

In general, FRP composites refers to the use of reinforcing fibers with a length of ¼" or greater. Recently, thermoplastic resins have been used with continuous fiber creating structural composite products. There are a few distinct advantages and disadvantages thermoplastic composites have against thermoset composites.

2.2.3. Advantages and disadvantages of thermoplastic resins

If we mention about two major advantages of thermoplastic resins, the first one is that many thermoplastic resins have an increased impact resistance to comparable thermoset composites. In some instances, the difference is as high as 10 times the impact resistance.

The other major advantage of thermoplastic composites is the ability reform. See, raw thermoplastic composites, at room temperature, are in a solid state. When heat and pressure impregnate a reinforcing fiber, a physical change occurs; not a chemical reaction as with a thermoset.

This allows thermoplastic composites to be reformed and reshaped. For example, a pultruded thermoplastic composite rod could be heated and remolded to have a curvature. This is not possible with thermosetting resins. This also allows for the recycling of the thermoplastic composite at end of life, in theory, not yet commercial.

Ofcourse there are some disadvantages of thermoplastic resins, a thermoplastic resin is naturally in a solid state, it is much more difficult to impregnate reinforcing fiber. The resin must be heated to the melting point, and pressure is required to impregnate fibers, and the composite must then be cooled under this pressure. This is complex and far different from traditional thermoset composite manufacturing.

Special tooling, technique, and equipment must be used, many of which is expensive. This is the major disadvantage of thermoplastic composites.

Advances in thermoset and thermoplastic technology are happening constantly. There is a place and a use for both, and the future of composites does not favor one over the other [31].

2.2.4. Ketone and aldehyde resins

Ketone and aldehyde resins are obtained by self-condensation or another word cocondensation between formaldehyde and aliphatic, cycloaliphatic, aliphatic-aromatic ketones or respectively aldehydes [32, 33]. In addition, further monomers, such as phenols and urea, also play a part. The aromatic hydrocarbon-formaldehyde resins are prepared from alkylated aromatic hydrocarbons, formaldehyde and sometimes other monomers.

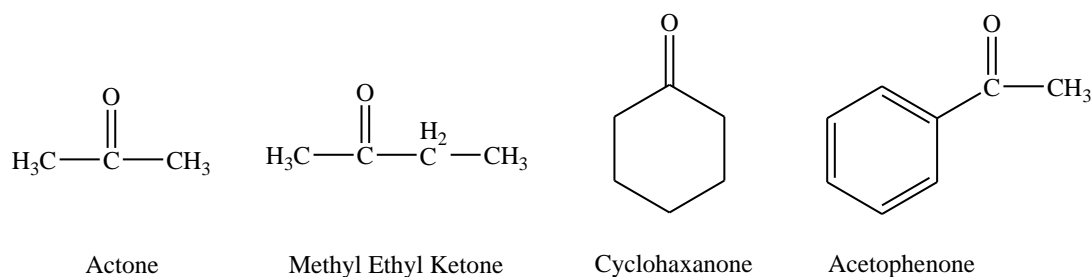
Although the resin groups involved have been known for a long time, their chemistry and applications remain areas of change even today. The following monomers are were given in Figure 2.2.

The resins are formed by polymerization of the vinyl ketones, giving polymers having an alternating structure or by complex condensation reactions of the methylol compounds with one another or with further ketone molecules, leading to partially branched oligomers. In industrial processes, the two mechanisms usually take place alongside one another. Excess formaldehyde may lead to the reduction of the carbonyl group-to hydroxyl groups [34]. Provided no substitution is carried out at the vinyl group, the polymerization activity of the vinyl ketone intermediate shows little dependence on the nature of the ketone employed [35, 36]. The industrial preparation of the resins is performed in reactors for condensation reactions, usually in a batchwise procedure.

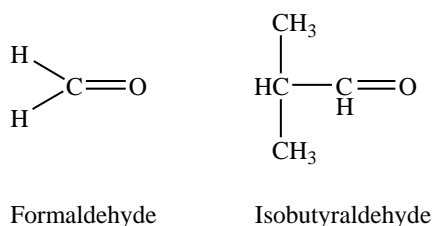
Ketone and aldehyde resins are employed in a large number of applications. In the coatings sector, as with most other applications, the products are used in combination with other binders, plasticizers, pigments and auxiliaries. The final formulations include marine paints, metal primers and wash primers, powder coatings and roadmarking paints. Among inks for printing and other purposes, mention may be made not only of

the well-established flexographic and gravure printing inks based on cellulose nitrate but also of transfer printing inks, radiation-curable systems and ink-jet inks. The ballpoint pastes produced nowadays are primarily based on hydrogenated acetophenone-formaldehyde resins. Further important applications are in recording and copying technology (toners), printed circuits, adhesives, binders for corrugated card, foundry moulding sands and laminates [37].

A. Ketones



B. Aldehydes



C. Allylated aromatics

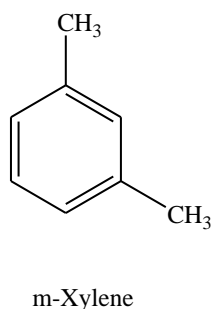


Figure 2.2: Monomers using in resin synthesis.

2.2.4.1. Aliphatic and cycloaliphatic ketone resins

Linear aliphatic ketones like methyl ethyl ketone and acetone are reacted to form resins with formaldehyde in particular. In the same way, methyl isobutyl ketone is

used to produce resins for adhesives. Higher aliphatic ketones no longer form resins. As regards the cycloaliphatic ketones, cyclohexanone and methylcyclohexanone are the most important, although cyclopentanone, cycloheptanone and cyclic ketones with longer side chains have been described as raw materials for resins. Some of these type resins will be illustrated further parts.

2.2.4.2. Methyl ethyl ketone formaldehyde resins

These resins are used in particular as binders for coatings and adhesives. They differ from resins based on cycloaliphatic or on aliphatic-aromatic ketones in their solubility and compatibility with other raw materials used in coatings. Their properties derive from the polarity of the ketone and from its specific behaviour during the alkaline-catalysed condensation.

The methyl ethyl ketone-formaldehyde resins possess a slight inherent coloration and are soluble in polar solvents such as alcohols, esters, ketones and glycol ethers. The resins are strongly polar, hygroscopic and have an oxygen content of from 21 to 29 per cent by mass. The molar masses are between 3000 and 5000 g/mol, the softening range between 80 and 125 °C.

The resins are prepared by alkaline-catalysed condensation of methyl ethyl ketone and formaldehyde in a molar ratio of from 1:2 to 1:2.5 in a batch process, Without purification beforehand, the ketone is reacted with formaldehyde in the presence of water. NaOH and KOH have proven to be the best catalysts for this reaction. The increase in the melting point from 80 to 120 °C can be achieved by raising the excess of formaldehyde. High softening points are also obtained by phase transfer catalysis. Special waning processes likewise lead to high-melting products which are light in colour [38].

The resins are often used together with film formers such as cellulose nitrate, acetylcellulose, cellulose ethers or natural resins. Among the properties endowed are, in particular, hardness, drying, sandability and good light stability. The resins possess the capacity to bring about gelatinization of cellulose nitrate. The free hydroxyl groups are explored for crosslinking in isocyanate two-pack coatings, in adhesives and in moulding sands [39].

2.2.4.3. Acetone formaldehyde resins

The alkaline-catalysed condensation of acetone and formaldehyde does not give rise to any solid synthetic resins which can be used. The substantially greater resinification tendency of the unstable methylolation stages of acetone [40, 41] leads to a crosslinked, insoluble final structure. However, self-curing precondensates can also be prepared, which can be employed alone or in combination with other curable precondensates, such as phenol resols. Water-soluble products are obtained when acetone and formaldehyde are reacted in a ratio of 1 to 3 [42]. These products can be crosslinked under alkaline conditions [43].

Rigid foams are obtained when the methylol compounds are foamed in the presence of alkali metal hydroxide, alone or in the presence of elastomer latex. In the production of mouldings, sands can be solidified using acetone-formaldehyde precondensates. Descriptions have also been given of quick-setting mouldings from cement. Acetone-formaldehyde condensation products find a wide variety of uses in the adhesive bonding of paper and of wood. In these applications, phenol resols are often cocondensed in order to obtain chipboard and wooden materials with particular weather resistance or to provide corrugated card with waterproof bonding. Further applications of acetone precondensates are as photoreceptors in electrophotography and for the production of additives [44].

2.2.4.4. Cyclohexanone resins

Cyclohexanone and methylcyclohexanone are also capable of self-condensation [45]. In this case an aldol condensation takes place between the carbonyl group and the activated methylene group of a second molecule. The carbonyl group of the intermediates reacts with a further molecule of cyclohexanone; similar reactions follow until the final product is formed. The reaction can be catalysed by basic, acidic or neutral agents, with potassium methylate being used most often.

The softening points are between 80 and 120 °C of the light-coloured, neutral resins. Under normal conditions the resins are resistant to acids and bases. But, under the action of acid they eliminate water at elevated temperatures (>80°C), and their properties are altered substantially. The cyclohexanone resins are lightfast, soluble

in many solvents and compatible with the majority of raw materials. They are more expensive than cyclohexanone-formaldehyde resins.

In coating materials, the primary functions of cyclohexanone resins are to improve full-ness, gloss and hardness. They may also increase the lightfastness and weather resistance and the adhesion. The resins are added in quantities of from 5 to 50 per cent by mass (based on the film former) to coating materials based on alkyd resins, vinyl chloride copolymers, chlorinated rubber, cellulose nitrate or oils. Their use as a carrier resin for pigment preparations has also been described. Reduction and partial esterification are possible ways to improve stability and flexibility. LaropalK80 (BASF) is an commercial product of an cyclohexanone resin [44, 46].

2.2.4.5. Cyclohexanone formaldehyde resins

Cyclohexanone can be reacted with aldehydes, especially formaldehyde, to give methylol compounds or resinous products. In this case it is the molar ratio and the reaction conditions which determine the properties of the end products. A high formaldehyde excess promotes the formation of methylol compounds, whereas basic catalysis leads to resin formation [45].

Higher aldehydes can likewise be used to produce resins, but have not found any industrial significance. On the other hand, methylcyclohexanone or mixtures with aliphatic ketones and, more recently, trimethylcy-clohexanone have been employed. The modification of the resins with phenols, epoxides, polyesters and sulphonamides is known. Small beads are obtained by addition of dispersants. The continuous preparation process has been described . Hydrogenation and treatment with reducing agents are ways in which the light stability can be increased.

Cyclohexanone-formaldehyde resins do not have the broad compatibility and solubility of the pure cyclohexanone resins. However, they are less expensive while being of adequate light stability. Although they can no longer be combined with oils, combination with a range of important paint binders is possible. The use of methylcyclo-hexanone as a raw material usually leads to enhanced solubility and compatibility. By using trimethylcyclohexanone, resins can be obtained whose compatibility and solubility are virtually universal.

A reaction which has become important for the industrial production of the resin is the condensation of cyclohexanone with formaldehyde in the presence of alkalis.

In many cases, the resins are used in order to improve drying, hardness, fullness, gloss and solids content. In coatings they are used in every case only as an accompaniment to other binders, for example in alkyd/acrylic coating materials, cement paints. Epoxy resin systems and marine paints. In addition to conventional printing ink, UV-curing printing inks also play an increasing role. A further principal area of application is represented by adhesives and sealing compounds. Another application which has been described is in optical recording media. The broad compatibility of resins based on trimethylcyclohexanone makes them ideally used to use in pigment pastes capable of universal application. Some examples of commercial resins are Kunstharz AFS (Bayer), Kunstharz CA (Hills), Kunstharz EP (Hills), Krumbhaar-Types (Lawter) and MR85 (A.O. Polymers) [46].

All the resins mentioned can be modified with many molecules for different purposes. Cyclohexanone-formaldehyde resins were in situ modified with using methyl isobutyl ketone, methyl ethyl ketone, methyl cyclohexanone, acetaldehyde, propion-aldehyde, cinnamaldehyde, dicyndiamide, arminotriazine and phenol [47, 48]. Also siloxane-containing block copolymers were investigated and reported. Many types of cyclohexanone-formaldehyde block copolymers with poly-siloxanes and their unique properties were reported [29, 49].

2.3. Nanocomposites

The term "nanocomposites" is a relatively new one in material science and is used to refer to a combination of two or more phases, where at least one dimension is in the nanometer size range. The parent phases may be inorganic, organic, or both, and may be amorphous, crystalline or semicrystalline. These types of materials are expected to exhibit new and improved catalytic, electronic, magnetic, and optical properties relative to both the parent phases and their corresponding micro- or macrocomposites. This synergistic behavior is a consequence of their ultrafine sizes and the existence of intra- or interphasic interactions [50].

Layered silicate-based polymer nanocomposites have demonstrated a significant potential to become the basis for development of the next generation of enhanced

performance polymer compounds. Incorporation of only a small loading (1 to 5%) of properly treated, well dispersed/exfoliated organoclay into the base polymer results in a compound with a substantial improvement in thermal, mechanical, as well as other physical properties over those of the base polymer. Until now, most development efforts have focused on determining proper surface treatment to make the clay compatible with the base polymer and therefore improve the ease with which it can be dispersed in the polymer. Most publications still concentrate on the importance of the chemistry used to modify the surface of the clay. They provide a description of resultant product properties but do not include the role of processing or give details of the compounding setup. Therefore, the key challenge facing many new entrants into the field is to determine how to maximize the clay exfoliation. Of course, using clay modified specifically for compatibility with the polymer matrix is extremely important; however, proper design and operation of the compounding system is equally critical [51].

Interest in nano-particle-based polymer composites has expanded significantly since the late 1980s when the patent of Okada et al. (assigned to Kabushiki Kaisha Toyota Chou Kenkyusho) for *in situ* polymerization of a Nylon 6/clay nanocomposite with, as stated in claim, “high mechanical strength and excellent high-temperature characteristics” was issued. The results presented in the patent show that polymer nanocomposites based on layered silicates provide a significant potential for development of a wide range of enhanced performance polymer compounds. As demonstrated by several researchers, a relatively small loading of properly dispersed (well-exfoliated) organoclay provides a substantial improvement in a polymer’s properties. These include improved thermal properties such as heat distortion temperature (HDT), mechanical properties such as flexural strength and modulus (without significant loss of impact), barrier properties, flame resistance, and abrasion resistance. However, until the early to mid 2000s, there were few commercial materials. Those in the market were mostly based on Nylon 6, and were for niche market applications. The reason for this, at least in part, is that many of the initial composites, such as the Toyota material previously noted, were developed using direct polymerization of a monomer clay mixture. While this method is suitable for certain polymers such as Polyamide 6, the complexity and expense of building a production facility limits entry of many smaller firms into the market [52-56].

2.3.1. Polymer / clay nanocomposites

Polymer nanocomposites are defined as polymers with nanometric fillers. The nanometric fillers are 1-100nm in size. Common polymer host matrices are nylon, polyepoxides, PDMS, LDPE, XLPE, PMMA, etc. Common inorganic filler particle candidates include MMT, TiO₂, ZnO, SiO₂, etc. An ideal nanocomposite should be free of any agglomerates and contain optimum filler content.

There are various methods to mix the polymer and filler particles. For thermoplastic polymers, such as polyethylene, filler particles are typically mixed into the polymer during melt mixing. For thermoset polymers, particles are normally added before or during polymerization. However, it is often very difficult to disperse nanoparticles well in polymers especially at a commercial production scale. Nanometric filler particles with high surface energy tend to agglomerate. In addition, hydrophilic nanoparticles and hydrophobic polymers are not compatible in nature. All these could affect particle dispersion in the polymer matrix and thus result in poor interfacial interaction [57, 58].

Conventional polymer composites are widely used in diverse applications, such as construction, transportation, electronics, and consumer products. Composites offer improved properties, including higher strength and stiffness, compared to pristine polymers. The properties of polymer composites are greatly affected by the dimension and microstructure of the dispersed phase. Nanocomposites are a new class of composites that have a dispersed phase with at least one ultrafine dimension, typically a few nanometers [59-61]. Nanocomposites possess special properties not shared by conventional composites, due primarily to large interfacial area per unit volume or weight of the dispersed phase (e.g., 750 m²/g). Clay layers dispersed at the nanoscale in a polymer matrix act as a reinforcing phase to form polymer clay nanocomposites, an important class of organic/inorganic nanocomposites.

These nanocomposites are also referred to as polymer–silicate nanocomposites and organic/inorganic hybrids. Polymer/clay nanocomposites can drastically improve mechanical reinforcement and high-temperature durability, provide enhanced barrier properties, and reduce flammability [62-64]. Clays that have a high aspect ratio of silicate nanolayers are desirable for polymer reinforcement. Montmorillonite filled

polymers are enjoying renewed interest, following publications of Toyota on nylon-clay nanocomposites [65, 66].

Colloid and surface chemistry play important roles in the synthesis of polymer/clay nanocomposites. Dispersion of clay layers in polymers is hindered by the inherent tendency to form face-to-face stacks in agglomerated tactoids due to high interlayer cohesive energy. Nanoscale dispersion of the clay tactoids into individual nanolayers is known as exfoliation or delamination. Exfoliation is further prevented by the incompatibility between hydrophilic clay and hydrophobic polymers. Treatment or functionalization of clay by adsorption of organic molecules weakens the interlayer cohesive energy. Intercalation, i.e., penetration of organic molecules into the clay interlayers, increases the compatibility between clay and polymer matrix. Due to the negative charge on the clay surface, cationic surfactants and polymers are commonly used for intercalation. The ion exchange of inorganic cations in clay galleries by organic cations renders the clay organophilic. Such organoclays have found large-scale applications for decades in cosmetics, drilling mud, paints, coatings, inks, and wastewater treatment. There is a growing interest in the surface chemistry of clays in pursuit of nanocomposite synthesis using specific monomers, prepolymers, and polymer melts [67].

2.3.2. Resin / clay nanocomposites

Contemporarily there are many types of resin/clay nanocomposites and it's still progressing day by day. The major types of resin/clay nanocomposites were elucidated below.

2.3.2.1. Epoxy resin nanocomposites

Clay mineral fillers, used for preparing nanocomposites based on epoxy matrices include layered double hydroxides, micas, and smectites. The common method used to obtain epoxy resin/ clay mineral nanocomposites is in-situ intercalative polymerization, based on dispersion of the clay within the epoxy resin followed by the addition of the hardener and subsequent curing. Studies on epoxy resin/montmorillonite nanocomposites were carried out with various types of epoxy resins, hardeners and systems with both exfoliated and intercalated particles were presented [68].

Last studies shows that organically modified clay reinforcement epoxy resins shows enhanced properties like elastic modulus, tensile strength, and impact toughness [69-71].

2.3.2.2. Phenolic resin nanocomposites

Phenolic resins, also called phenolic plastics or phenoplasts, were among the first synthetic resins composed by deliberate synthesis and are therefore among the earliest synthetic binders of any kind. Consequently, it is hardly surprising that the reaction mechanisms in the synthesis of these resins and their reactions with other substances have been the subject of particularly intense study.

Phenolic resins are produced by the reaction of phenol with aldehyde and are classified as resol and novolac by synthetic conditions and curing mechanism. It is very difficult to synthesize a phenolic resin/layered silicate nanocomposite, since phenolic resin has three-dimensional structure, even if it is not cross-linked [72].

Usuki et al. [73] tried to synthesize phenolic resin/layered silicate nanocomposite by intercalative polymerization of phenolic resin with phenol and formaldehyde in the presence of oxalic acid and montmorillonite modified with 4-aminophenol hydrochloride. Resol type phenolic resins was not studied in the polymer/layered silicate nanocomposite field because of difficulty in making linear resol type phenolic oligomers at the time.

Choi et al. [74, 75] synthesized phenolic resin/layered silicate nanocomposites by the melt intercalation of linear novolac with intercalated or exfoliated nanostructures by melt intercalation using linear novolac.

Kızılcan et al. [76] synthesized phenolic resin/layered silicate nanocomposites by in situ technique with direct addition of DH-PDMS and pristine clay molecules and achieved better thermal and mechanical properties. Nanocomposites were obtained which can be used for thermal insulation materials, coatings, molding compounds and aerospace components.

2.3.2.3. Urea formaldehyde resin nanocomposites

Urea formaldehyde resins are the products of condensation reaction of formaldehyde with urea containing two amine groups, under basic or acid conditions. Urea formaldehyde resins are the most prominent examples of the class of surface-coating

thermosetting resins usually referred to as amino resins. The excellent color retention, hardness, and chemical resistance of the urea formaldehyde resins are transmitted to the coating system [77].

Lei et al. [78] reported that the addition of small percentages of Na⁺-montmorillonite (NaMMT) nanoclay appears to considerably improve the performance of thermosetting urea formaldehyde (UF) resins used as adhesives for plywood and for wood particleboard. The influence of NaMMT addition was particularly noted in plywood by the increase in water resistance of the UF-bonded panel.

Kızılcan et al. [79] reported that T_g-T_m region of some nanocomposites is enhanced and by assessing the results of hardness measurements, it is concluded that these samples have further improved mechanical properties as a coating material than urea formaldehyde resin have.

2.3.3. Nanocomposite preparation

Several strategies have been considered to prepare polymer-layered silicate nanocomposites.

They include four main processes [80]:

a) In situ intercalative polymerization: In this technique, the layered silicate is swollen within the liquid monomer (or a monomer solution) so as the polymer formation can occur in between the intercalated sheets. Polymerization can be initiated either by heat or radiation, by the diffusion of a suitable initiator or by an organic initiator or catalyst fixed through cationic exchange inside the interlayer before the swelling step by the monomer.

b) Exfoliation adsorption: The layered silicate is exfoliated into single layers using a solvent in which the polymer (or a prepolymer in case of insoluble polymers such as polyimide) is soluble. It is well known that such layered silicates, owing to the weak forces that stack the layers together can be easily dispersed in an adequate solvent. The polymer then adsorbs onto the delaminated sheets and when the solvent is evaporated (or the mixture precipitated), the sheets reassemble, sandwiching the polymer to form, in the best case, an ordered multilayer structure. Under this process are also gathered the nanocomposites obtained through emulsion polymerization where the layered silicate is dispersed in the aqueous phase.

c) Melt intercalation: The layered silicate is mixed with the polymer matrix in the molten state. Under these conditions and if the layer surfaces are sufficiently compatible with the chosen polymer, the polymer can crawl into the interlayer space and form either an intercalated or an exfoliated nanocomposite. In this technique, no solvent is required.

d) Template synthesis: This technique, where the silicates are formed in situ in an aqueous solution containing the polymer and the silicate building blocks has been widely used for the synthesis of double-layer hydroxide-based nanocomposites but is far less developed for layered silicates. In this technique, based on self-assembly forces, the polymer aids the nucleation and growth of the inorganic host crystals and gets trapped within the layers as they grow.

2.3.4. Nanoparticle dispersion in polymers

There are three main dispersion way for nanoparticles in polymers [81, 82]. These are non-intercalated, intercalated and exfoliated which is illustrated in Figure 2.3.

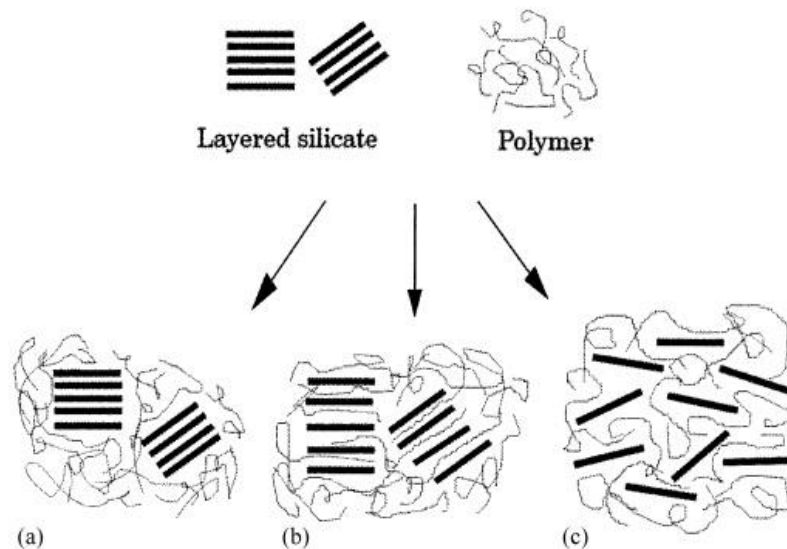


Figure 2.3: Dispersion of nanoparticles in polymers [81, 82].

a) Non-intercalated: In this case, the clay tactoids are dispersed simply as a segregated phase, resulting in poor mechanical properties of the composite. When the polymer is unable to intercalate between the silicate sheets, a phase separated composite is obtained, whose properties stay in the same range as traditional microcomposites.

b) Intercalated: In intercalated nanocomposites, the insertion of a polymer matrix into the layered silicate structure occurs in a crystallographically regular fashion, regardless of the clay to polymer ratio. Intercalated nanocomposites are normally interlayer by a few molecular layers of polymer. Properties of the composites typically resemble those of ceramic materials.

c) Exfoliated: When the silicate layers are completely and uniformly dispersed in a continuous polymer matrix, an exfoliated or delaminated structure is obtained. In an exfoliated nanocomposite, the individual clay layers are separated in a continuous polymer matrix by an average distances that depends on clay loading. Usually, the clay content of an exfoliated nanocomposite is much lower than that of an intercalated nanocomposite. Exfoliation is particularly desirable for improving specific properties that are affected by the degree of dispersion and resulting interfacial area between polymer and clay nanolayers.

Homogeneous dispersion of clay nanolayers in a polymer matrix provides maximum reinforcement via distribution of stress and deflection of cracks resulting from an applied load. Interactions between exfoliated nanolayers with large interfacial area and surrounding polymer matrix lead to higher tensile strength, modulus, and thermal stability. Conventional polymer–filler composites containing micron-size aggregated tactoids also improve stiffness, but at the expense of strength, elongation, and toughness. However, exfoliated clay nanocomposites of Nylon-6 and epoxy have shown improvements in all aspects of thermomechanical behavior. Exfoliation of silicate nanolayers with high aspect ratio also provides other performance enhancements that are not achievable with conventional particulate composites. The impermeable clay nanolayers provide a tortuous pathway for a permeant to diffuse through the nanocomposite. The hindered diffusion in nanocomposites leads to enhanced barrier property, reduced swelling by solvent, and improvements in chemical stability and flame retardance [83].

2.3.5. Montmorillonite

For preparing polymer–clay nanocomposites, commonly using clays are belong to the 2:1 layered structure type. A member of the 2:1 family, montmorillonite is one of the most interesting and widely investigated clays for polymer nanocomposites. The structure of montmorillonite consists of layers made up of one octahedral alumina

sheet sandwiched between two tetrahedral silica sheets, as shown in Figure 2.4. Stacking of the silicate layers leads to a regular van der Waals gap between the layers. Approximately one in six of the aluminum ions in the octahedral layers of montmorillonite is isomorphously substituted by magnesium or other divalent ions. The isomorphous substitution renders negative charges that are counterbalanced by cations residing in the interlayer. Pristine clay usually contains hydrated inorganic cations such as Na^+ , K^+ , and Ca^{+2} . When the inorganic cations are exchanged by organic cations, such as from surfactants and polyelectrolytes, the clay surface changes from hydrophilic to hydrophobic or organophilic. The organic cations lower the surface energy and decrease the cohesive energy by expanding the interlayer distance, thus facilitating the wetting and intercalation of monomer or polymer. In addition, the organic cations may contain various functional groups that react with monomer or polymer resin to improve interfacial adhesion between clay nanolayers and polymer matrix [84].

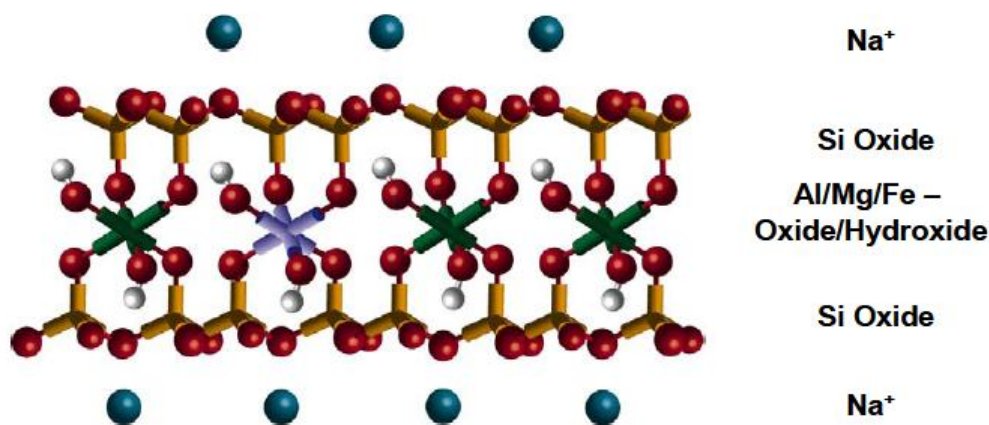


Figure 2.4: Montmorillonite structure T: Tetrahedral sheet; O: Octahedral sheet [84].

2.2.6. Agglomeration of nanoparticles in polymer matrix

Aggregates are particles combined by covalent bonds. Agglomerates are particles held together by van der Waals attraction and polar bonds. However, the literature is very large and often uses contradictory terminology. Prior to establishing the above terminology, the term “aggregation” was used to include gelling, coagulation, flocculation, and coacervation (liquid precipitation). Small particles tend to agglomerate. This is due to inter-particle attractive forces. As the particle sizes decrease, the surface area becomes large relative to mass. The large surface areas

include agglomeration. This tendency is much greater for polar particles such as oxides (SiO_2 , TiO_2 , etc.) and carbonates (CaCO_3) than for nonpolar particles such as carbon black. When polar particles are suspended in polar media containing ions, they tend to accumulate ions on their surfaces, making them electrically charged. At the negative charged colloidal particle surface, counter-ions accumulate and form an electrical doublelayer, called the Stern layer and the diffuse layer. The electrostatic potential is highest at the particle surface and decreases as distance from it increases. Charged particles with counter-ions repel each other, while uncharged particles attract each [85].

3. EXPERIMENTAL PART

3.1. Materials

Cyclohexanone and formaldehyde solution (37%) were supplied by Riedel-de Haen and LAB-SCAN respectively for synthesis of cyclohexanone formaldehyde resin. Sodium hydroxide pellets were supplied by Riedel-de Haen. The nanofiller, sodium-montmorillonite (MMT) (Nanofil 757) was used from Süd-Chemie (Switzerland). It is a highly purified natural sodium montmorillonite with cation-exchange capacity of 80 meq/100 g,m medium particle size as $<10\ \mu\text{m}$, and bulk density of approximately $2.6\ \text{g cm}^{-3}$. α,ω - diamine poly(dimethylsiloxane) (DA.PDMS) was the product of Sigma-Aldrich (Germany). Molecular weight of DA.PDMS was 1000 ± 80 .

3.2. Synthesis of Cyclohexanone Formaldehyde Resin (CFR)

98 g (1 mol) of cyclohexanone, 25 ml of cyclohexane and 30 ml of 37% formalin were put into a three-necked flask equipped with a stirrer and a condenser. When the temperature of the mixture was raised to $70\text{-}80\ ^\circ\text{C}$, refluxing started, subsequently, 100 ml of 37% formaline was added. As a catalyst NaOH solution (20 wt%) was used. The reaction was further continued under pH values of 11-12 for 5h. After reaction time was completed, two layers were formed. The resin was separated and purified by decanting the water layer and washed several times with warm water until it was free from then it was dried at 100°C in vacuumed oven.

3.3. Synthesis of DA.PDMS Modified Cyclohexanone Formaldehyde Resin (DA.PDMS-CFR)

98 g (1 mol) of cyclohexanone, 25 ml of cyclohexane, 30 ml of 37% formalin and 2 wt% of DA.PDMS were put into a three-necked flask equipped with a stirrer and a condenser. When the temperature of the mixture was raised to $70\text{-}80\ ^\circ\text{C}$, refluxing started, subsequently, 100 ml of 37% formaline was added. The reaction was further continued under pH values of 11-12 for 5h. After reaction time was completed, two

layers were formed. The resin was separated and purified by decanting the water layer and washed several times with warm water until it was free from, then it was dried at 100°C in vacuumed oven.

3.4. Synthesis of Layered Clay Nanocomposites of Cyclohexanone Formaldehyde Resin Samples (LC-CFR)

LC-CFR samples were synthesized in initially fed four different clay contents of several weight fractions (0,5 wt%, 1 wt%, 1,5 wt%, 3 wt%). Unmodified montmorillonite (pristine) clay was used to prepare resin/clay nanocomposites. 98 g (1 mol) of cyclohexanone, 25 ml of cyclohexane, 30 ml of 37% formalin and desired clay content were put into a three-necked flask equipped with a stirrer and a condenser. When the temperature of the mixture was raised to 70-80 °C, refluxing started, subsequently, 100 ml of 37% formaline was added. As a catalyst NaOH solution (20 wt%) was used. The reaction was further continued under pH values of 11-12 for 5h. After reaction time was completed, two layers were formed. The resin was separated and purified by decanting the water layer and washed several times with warm water until it was free from, then it was dried at 100°C in vacuumed oven. Final samples were named with reference to their clay contents. Clay contents of resin samples are given below on the Table 3.1.

Table 3.1: Contents of LC-CRF nanocomposite samples.

Resins	Clay content wt%	C:F molar ratio
LC-CFR1	0,5	1:1.6
LC-CFR2	1	1:1.6
LC-CFR3	1,5	1:1.6
LC-CFR4	3	1:1.6

3.5. Synthesis of DA.PDMS Modified Layered Clay Nanocomposites of Cyclohexanone Formaldehyde Resin (DA.PDMS-LC-CFR)

DA.PDMS-LC-CFR samples were synthesized in four different initial feed clay contents by weight (0,5 wt%, 1 wt%, 1,5 wt%, 3 wt%). Unmodified montmorillonite clay was used to prepare resin/clay nanocomposites. 98 g (1 mol) of cyclohexanone,

25 ml of cyclohexane, 30 ml of 37% formalin, 2 wt% of DA.PDMS and desired clay content were put into a three-necked flask equipped with a stirrer and a condenser. When the temperature of the mixture was raised to 70-80 °C, refluxing started, subsequently, 100 ml of 37% formaline was added. As a catalyst NaOH solution (20 wt%) was used. The reaction was further continued under pH values of 11-12 for 5h. After reaction time was completed, two layers were formed. The resin was separated and purified by decanting the water layer and washed several times with warm water until it was free from, then it was dried at 100°C in vacuumed. Final samples named with reference to their clay contents. Clay and PDMS contents of resin samples are given below on the Table 3.2.

Table 3.2: Contents of DA.PDMS-LC-CRF nanocomposite samples.

Resin Sample	Clay content wt%	DA.PDMS content wt%	C:F molar ratio
DA.PDMS-LC-CFR1	0,5	2	1:1.6
DA.PDMS-LC-CFR2	1	2	1:1.6
DA.PDMS-LC-CFR3	1,5	2	1:1.6
DA.PDMS-LC-CFR4	3	2	1:1.6

3.6. Characterization of CFR, DA.PDMS-CFR, LC-CFR and DAPDMS-LC-CFR Samples

FT-IR spectra was measured using model recorded Perkin-Elmer Spectrum One FT-IR (ATR sampling accessory) spectrophotometer, directly from the sample without help of the KBr discs.

¹H-NMR data were obtained from a Varian (AC 500 MHz, Germany) spectrometer, using CD₂Cl₂ as solvent and TMS as internal reference.

DSC thermograms were obtained by using Perkin-Elmer DSC-6 instrument (USA); the heating rate was 10 °C/min starting from 30 °C under a nitrogen atmosphere.

TGA was carried out in nitrogen atmosphere at a heating rate 10 °C/min up to 800 °C temperature by Perkin-Elmer Pyris 1. Weight loss (%) of samples was calculated at temperature range 20-760 °C.

XRD results were obtained by using Rigaku D/Max-Ultima+/PC XRD instrument. Scanning rate was 10° to 70°.

Morphology of products was examined by scanning electron microscope, ESEM XL30 ESEM-FEG Philips and the samples for the SEM measurement are prepared by gold coating.

4. RESULT AND DISCUSSION

4.1. Reaction Mechanism and Characterization of CFR

The formation of CF resin starts with an aldol-like reaction. Reaction follows a base catalyzed elimination reaction of water from methylol derivatives of cyclohexanone [86, 87]. Then methylol derivatives of cyclohexanones are joining together and polymerizing with monomers in the reaction media. The final product, CF resin, is obtained with the polymerization between them. The figure of the reaction mechanism illustrated below.

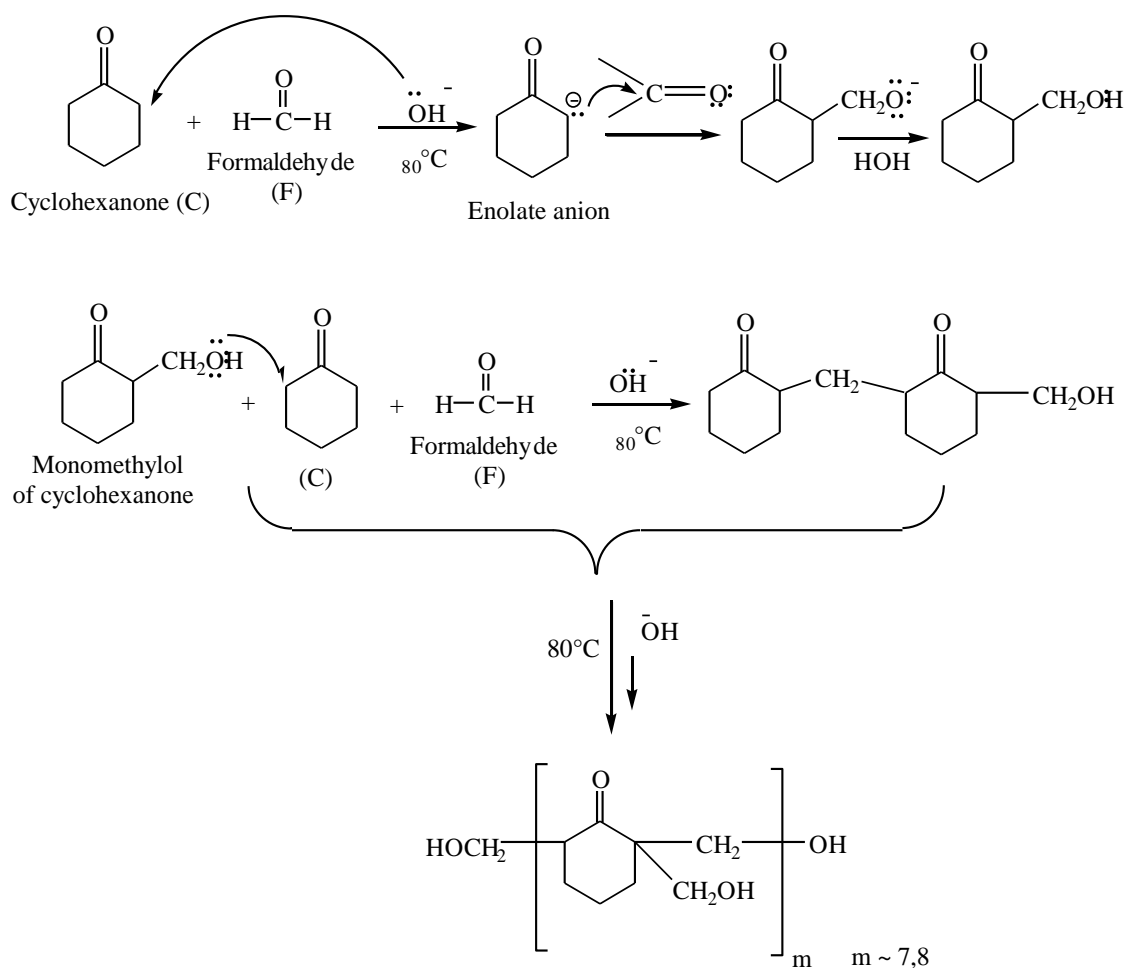


Figure 4.1: Reaction mechanism of CFR.

4.1.1. $^1\text{H-NMR}$ spectroscopy of CFR

The $^1\text{H-NMR}$ spectra were recorded from the deuterated solvent solution which is CD_2Cl_2 . In Figure 4.2, the peaks were appeared at about 1.1 – 2.4 ppm were due to the aliphatic $-\text{CH}_2$ and $-\text{CH}$ groups, 3.2 – 4.2 ppm due to the $-\text{CH}_2$ methylen bridges and methyl groups, 4.5 – 4.8 ppm due to the $-\text{OH}$ groups of the methyl groups [88].

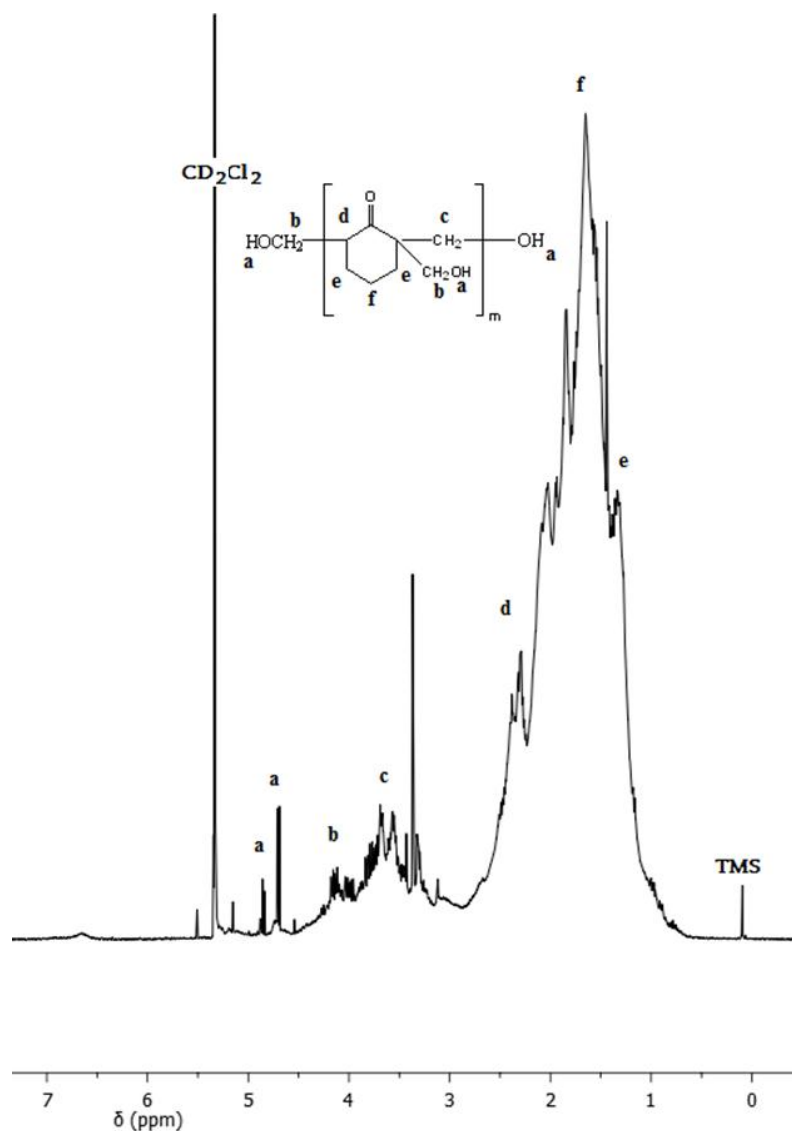


Figure 4.2: $^1\text{H-NMR}$ spectrum of CFR.

4.1.2. FTIR-ATR spectroscopy of CFR

According to the previous studies, characteristic peaks of cyclohexanone formaldehyde resin are 3400 cm^{-1} , 2920 cm^{-1} , 1700 cm^{-1} and 1450 cm^{-1} [78, 89].

In this study, these characteristic peaks were observed at 3399 cm^{-1} , 2925 cm^{-1} , 1699 cm^{-1} and 1445 cm^{-1} . These peaks respectively attributed to hydroxy methyl groups, aliphatic $-\text{CH}_2$, carbonyl $\text{C}=\text{O}$, and $-\text{CH}_2$ methylene bridges. Also between $970\text{--}1200$

cm^{-1} three main peaks were observed which belongs to the C-O stretch between methylene bridges and cyclohexanone ring. The spectrum of the synthesized pure resin was given in the Figure 4.3. These characteristic wavelenghts of the pure CF resin and observed wavelenghts of the pure CF resin were given in the Table 4.1.

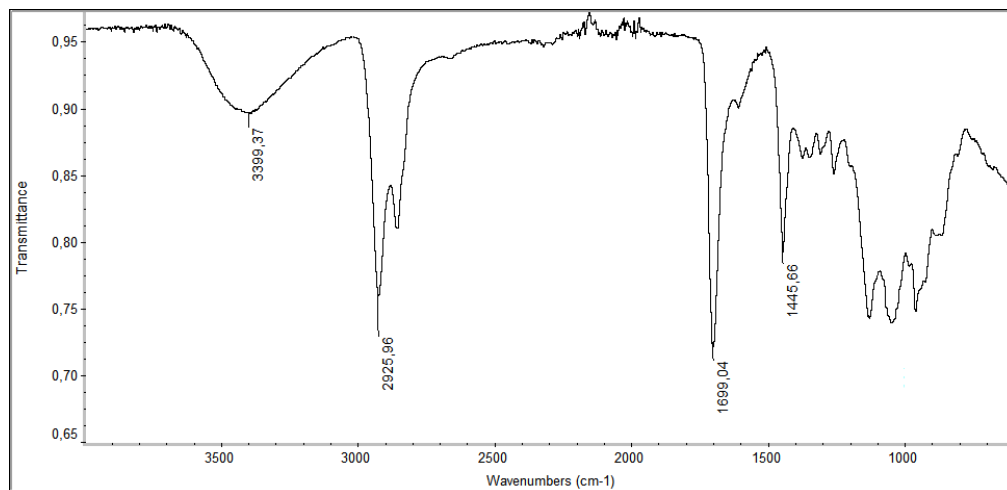


Figure 4.3: FTIR spectrum of CFR.

Table 4.1: Characteristic literature wavenumber values and observed wavenumber values of of CFR.

CFR		
Literature wavenumber values, cm^{-1}	Observed wavenumber values, cm^{-1}	Functional group
3400	3399	-OH
2920	2925	Aliphatic -CH ₂
1700	1699	Carbonyl C=O
1450	1445	-CH ₂ methylene bridge

4.1.3. DSC thermal analysis of CFR

DSC results of CFR was operated with one cycle. The cycle was heated 30°C to 300° with $10^{\circ}/\text{min}$ heating rate. In the literature T_g value of CFR is about 30°C [90]. In this study, as it is seen in the Figure 4.4, T_g value of CFR was determined as 45°C .

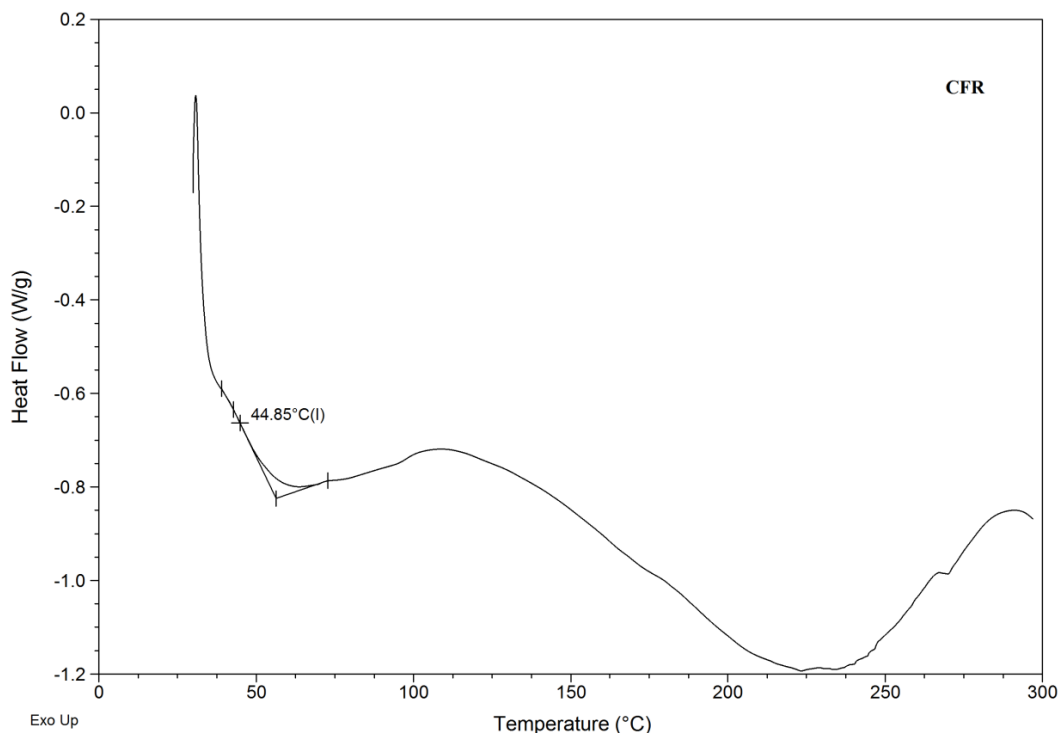


Figure 4.4: DSC thermogram of CFR.

4.2. Reaction Mechanism and Characterization of DA.PDMS-CFR

The formation of DA.PDMS-CFR resin starts with an aldol-like reaction. Reaction follows a base-catalyzed elimination reaction of water from methylol derivatives of cyclohexanone. As a result of the reaction between formaldehyde and amine chain ended PDMS (bis(3-aminopropyl) terminated), dimethylol PDMS molecules is occurred. Then methylol derivatives of cyclohexanones are joining together and polymerizing with monomers and dimethylol PDMS molecules in the reaction media. The final product, DA.PDMS-CF resin, is obtained with the polymerization between them. Diamine polydimethylsiloxanes with an amine chain end probably acted as an amine component of the Mannich type reaction under the conditions of the resin preparation. Because the molar ratio of formaldehyde to amine was rather high, each $-NH_2$ groups should have reacted with 2 mol of formaldehyde and 2 mol of ketones. The intermediate formed from aldol-like reactions and Mannich type reactions combined by the effect of the base catalyst to form modified resin similar to base-catalyzed ketonic resin formation [29, 91]. The figure of the reaction mechanism illustrated on Figure 4.5.

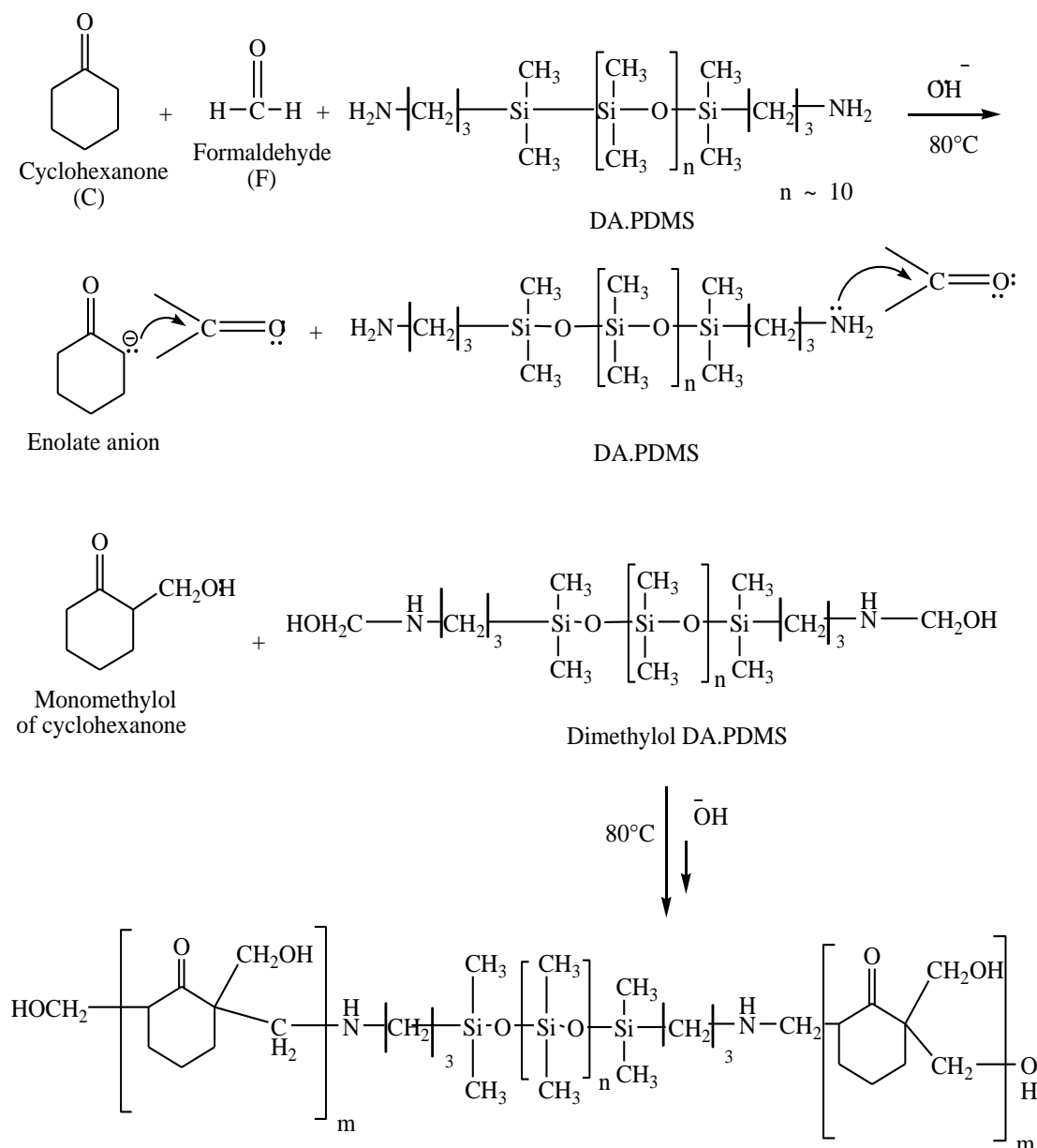


Figure 4.5: Reaction mechanism of DA.PDMS-CFR.

4.2.1. $^1\text{H-NMR}$ spectroscopy of DA.PDMS-CFR

The $^1\text{H-NMR}$ spectra were recorded from the deuterated solvent solution which is CD_2Cl_2 . In Figure 4.6, the peaks were appeared at about 1.1 – 2.4 ppm were due to the aliphatic $-\text{CH}_2$ and $-\text{CH}$ groups, 3.2 – 4.2 ppm due to the $-\text{CH}_2$ methylen bridges and methyl groups, 4.5 – 4.8 ppm due to the $-\text{OH}$ groups of the methyl groups [88].

The peaks are appearing at about 0.05– 0.1 ppm due to $-\text{Si-CH}_2$ and Si-CH_3 groups, 0.9 – 1 ppm due to $-\text{NH}$ groups because of DA.PDMS [29].

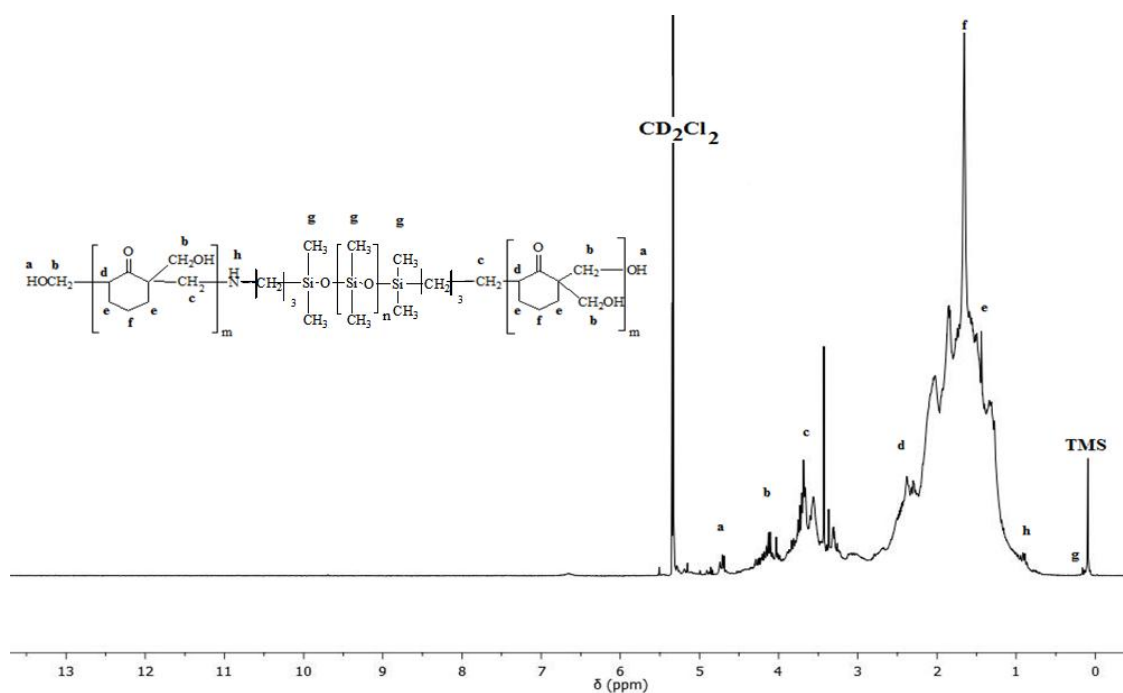


Figure 4.6: $^1\text{H-NMR}$ spectrum of DA.PDMS-CFR.

4.2.2. FTIR-ATR spectroscopy of DA.PDMS-CFR

Previously, characteristic peaks of cyclohexanone formaldehyde resin were mentioned. When examining the DA.PDMS-CFR, in addition of the CFR, $860\text{-}760\text{cm}^{-1}$ peaks and increase in absorbance level at $1000\text{-}1100\text{ cm}^{-1}$ were observed. These peaks respectively belong to Si-CH₃ groups and Si-O-Si groups [29]. Because of -CH vibrations between $1150\text{-}750\text{ cm}^{-1}$, these Si-CH₃ and Si-O-Si vibrations are barely noticeably on the spectrum, but the intensity is getting stronger with addition of DA.PDMS to the samples.

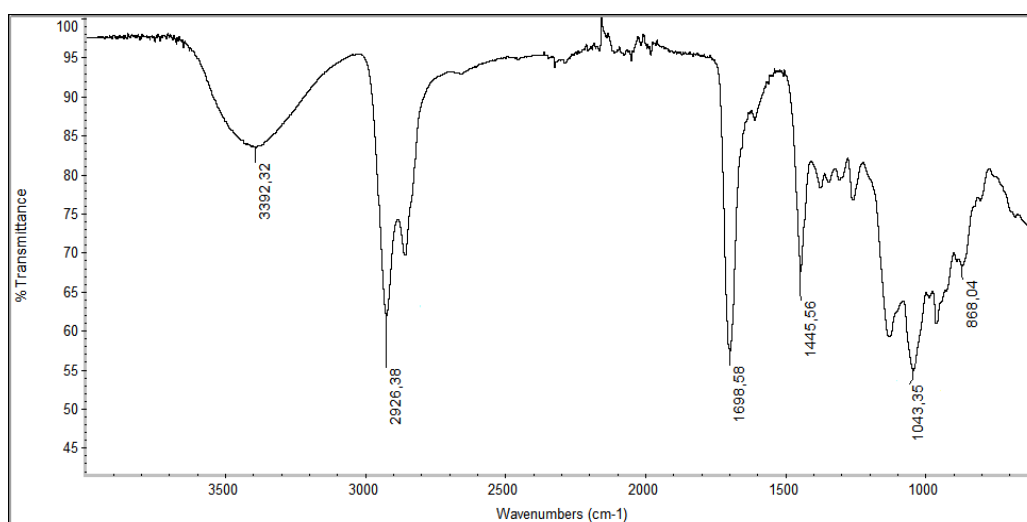


Figure 4.7: FTIR spectrum of DA.PDMS-CFR.

In this study, characteristic peaks were observed at 3392 cm^{-1} , 2926 cm^{-1} , 1698 cm^{-1} , 1445 cm^{-1} , 1043 cm^{-1} and 868 cm^{-1} . These peaks respectively attributed to hydroxy methyl groups, aliphatic $-\text{CH}_2$, carbonyl $\text{C}=\text{O}$, $-\text{CH}_2$ methylene bridge, Si-O-Si groups and Si- CH_3 groups. The spectrum of the synthesized DA.PDMS-CFR was given in the Figure 4.7. These characteristic wavenumbers of the DA.PDMS-CFR and observed wavenumbers of the pure DA.PDMS-CFR were given in the Table 4.2.

Table 4.2: Characteristic literature wavenumber values of DA.PDMS-CFR and observed wavenumber values of DA.PDMS-CFR.

DA.PDMS-CFR		
Literature wavenumber values, cm^{-1}	Observed wavenumber values, cm^{-1}	Functional group
3400	3392	-OH
2920	2926	Aliphatic $-\text{CH}_2$
1700	1698	Carbonyl $\text{C}=\text{O}$
1450	1445	Methylene bridge $-\text{CH}_2$
1000-1100	1043	Si-O-Si groups
860-800	868	Si- CH_3 groups

4.2.3. DSC thermal analysis of DA.PDMS-CFR

DSC results of DA.PDMS-CFR was operated with one cycle. The cycle was heated 30°C to 300° with $10^\circ/\text{min}$ heating rate. As it was seen in the Figure 4.8, it is realized that, T_g value of DA.PDMS-CFR is higher than the pure CFR and it was determined as 68° .

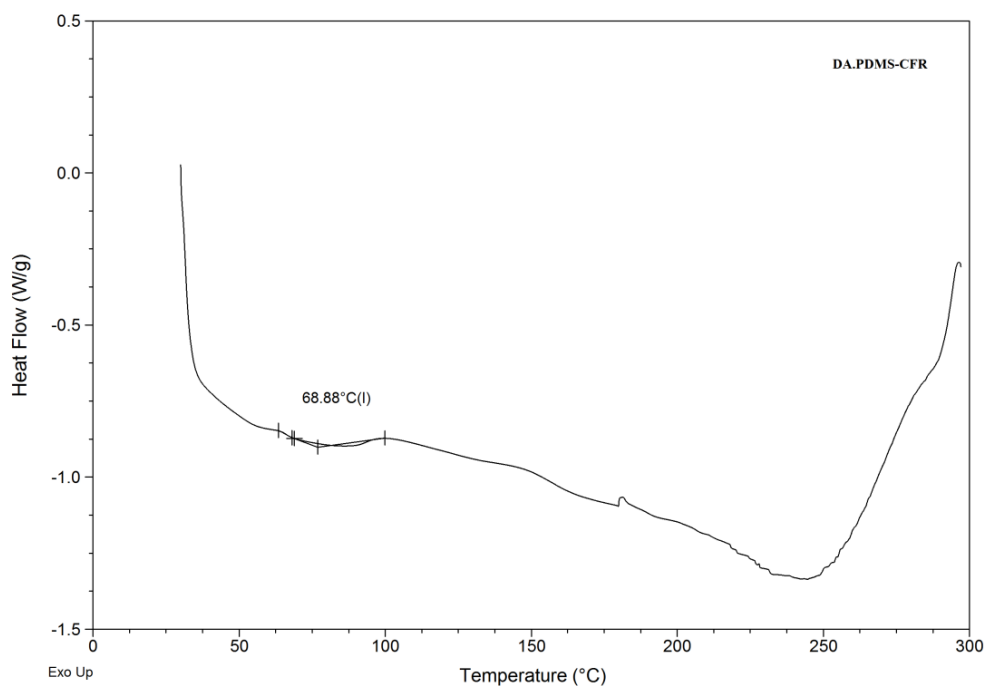


Figure 4.8: DSC thermogram of DA.PDMS-CFR.

4.3. Characterization of MMT Clay

4.3.1. FTIR-ATR spectroscopy of MMT clay

As it is seen in the Figure 4.9, characteristic peaks of MMT clay was observed at 3635 cm^{-1} , 1631 cm^{-1} , 992 cm^{-1} , 795 cm^{-1} and 764 cm^{-1} . According to the literature [92-94], these peaks attributed to O-H stretching vibration of structural -OH, bending vibration of -OH in water (moisture), stretching of Si-O-Si bonds and final two peaks attributed to deformation of Si-O-Si bonds.

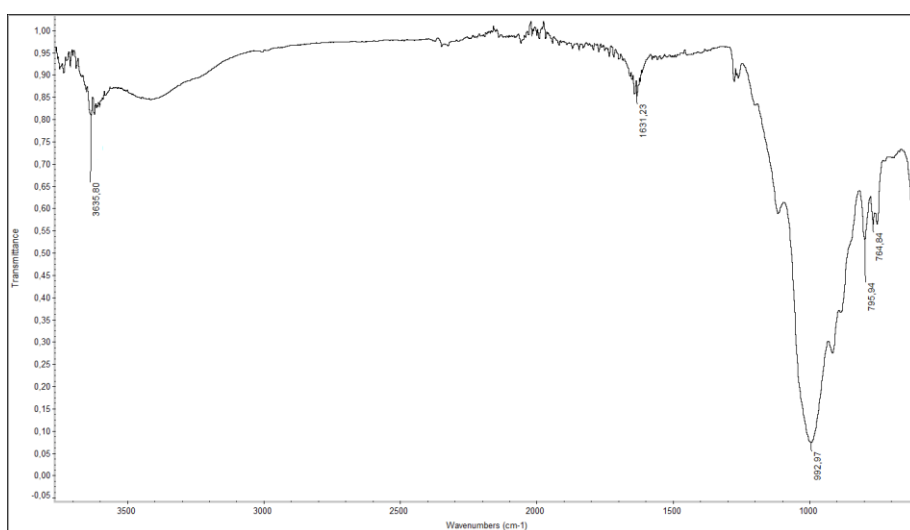


Figure 4.9: FTIR spectrum of MMT clay.

4.3.2. XRD analysis of MMT clay

By using Bragg equation, the distances between clay sheets of neat clay and resin/clay nanocomposites are calculated from their XRD test results. Wavelength of radiation (λ) used was 0,7698 Å.

Bragg equation: $\lambda = 2d \sin\theta$

As it is seen in the equation, if 2θ values (diffraction angles) would be put into the equation to their positions, the distances (d) between sheets of clays (d_{001} spacings, basal spacings) can be calculated easily.

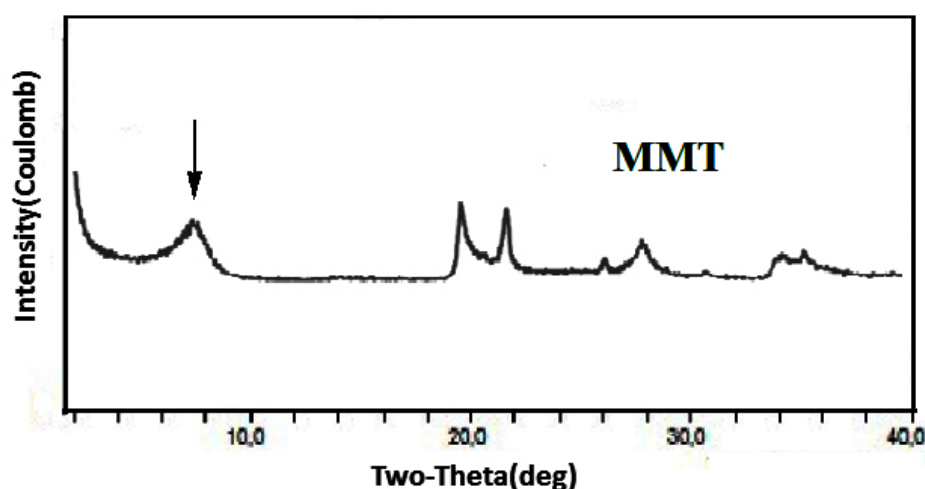


Figure 4.10: XRD pattern of MMT clay.

As it seen in the Figure 4.10, the 2θ value of neat montmorillonite clay used was found at 7.3° . If the value put into the Bragg equation to its position, the basal spacing of neat MMT can be found as 12.2 Å. Further XRD results of nanocomposites can be calculated by using this equation with using their 2θ values from their test results.

4.4. Characterization of LC-CFR Nanocomposite Samples

4.4.1. FTIR-ATR spectroscopy of LC-CFR nanocomposite samples

The FTIR spectrum of LC-CFR1 was illustrated in Figure 4.11 and the characteristic peaks of LC-CFR1 were observed at 3402 cm^{-1} , 2926 cm^{-1} , 1698 cm^{-1} , 1445 cm^{-1} , 1044 cm^{-1} and 749 cm^{-1} . These peaks respectively attributed to hydroxy methyl

groups, aliphatic $-\text{CH}_2$, carbonyl $\text{C}=\text{O}$, $-\text{CH}_2$ methylene bridges, stretching of Si-O-Si of MMT and deformation of Si-O-Si of MMT.

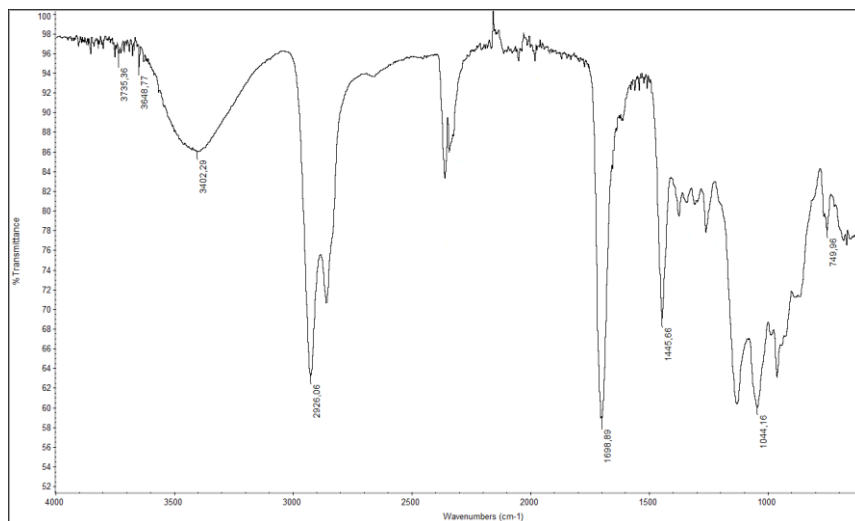


Figure 4.11: FTIR spectrum of LC-CFR1.

The FTIR spectrum of LC-CFR2 was illustrated in Figure 4.12 and the characteristic peaks of LC-CFR2 were observed at 3398 cm^{-1} , 2926 cm^{-1} , 1704 cm^{-1} , 1445 cm^{-1} , 1051 cm^{-1} and 749 cm^{-1} . These peaks respectively attributed to hydroxy methyl groups, aliphatic $-\text{CH}_2$, carbonyl $\text{C}=\text{O}$, $-\text{CH}_2$ methylene bridges and stretching of Si-O-Si of MMT.

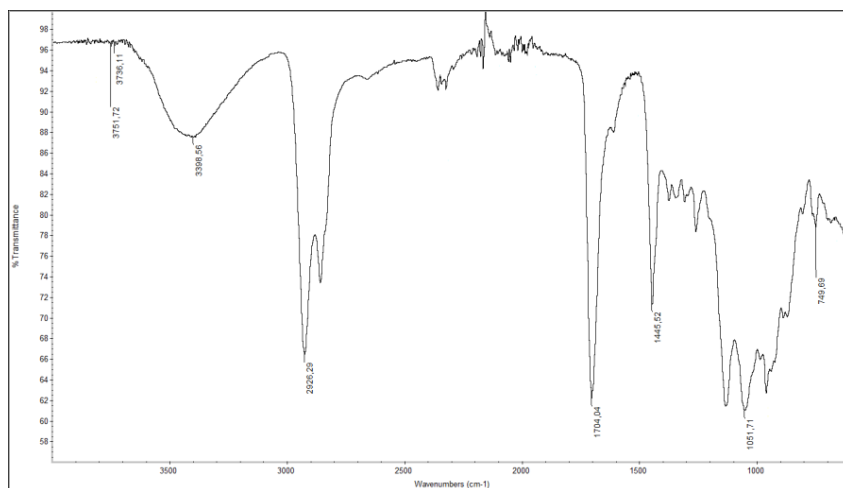


Figure 4.12: FTIR spectrum of LC-CFR2.

The FTIR spectrum of LC-CFR3 was illustrated in Figure 4.13 and the characteristic peaks of LC-CFR3 were observed at 3390 cm^{-1} , 2927 cm^{-1} , 1698 cm^{-1} , 1445 cm^{-1} , 1051 cm^{-1} and 750 cm^{-1} . These peaks respectively attributed to hydroxy methyl groups, aliphatic $-\text{CH}_2$, carbonyl $\text{C}=\text{O}$, $-\text{CH}_2$ methylene bridges and stretching of Si-O-Si of MMT.

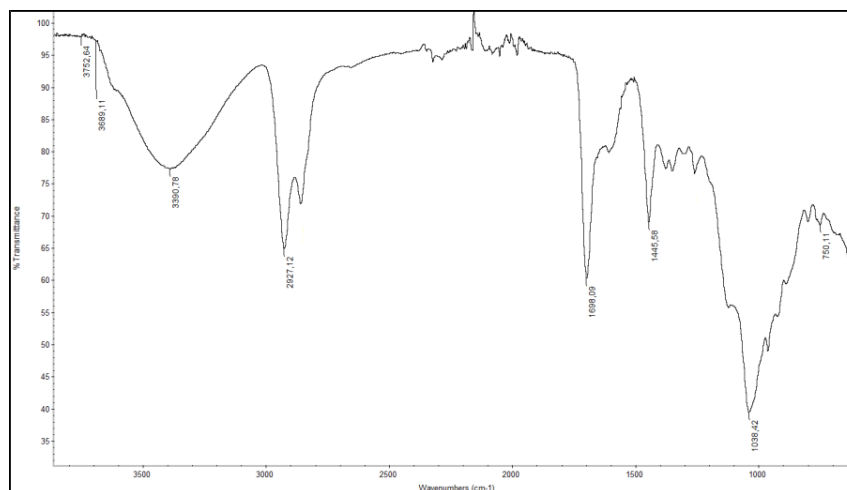


Figure 4.13: FTIR spectrum of LC-CFR3.

The FTIR spectrum of LC-CFR4 was illustrated in Figure 4.14 and the characteristic peaks of LC-CFR4 were observed at 3339 cm^{-1} , 2926 cm^{-1} , 1703 cm^{-1} , 1445 cm^{-1} , 1041 cm^{-1} and 747 cm^{-1} . These peaks respectively attributed to hydroxy methyl groups, aliphatic $-\text{CH}_2$, carbonyl $\text{C}=\text{O}$, $-\text{CH}_2$ methylene bridges, stretching of Si-O-Si of MMT and deformation of Si-O-Si of MMT.

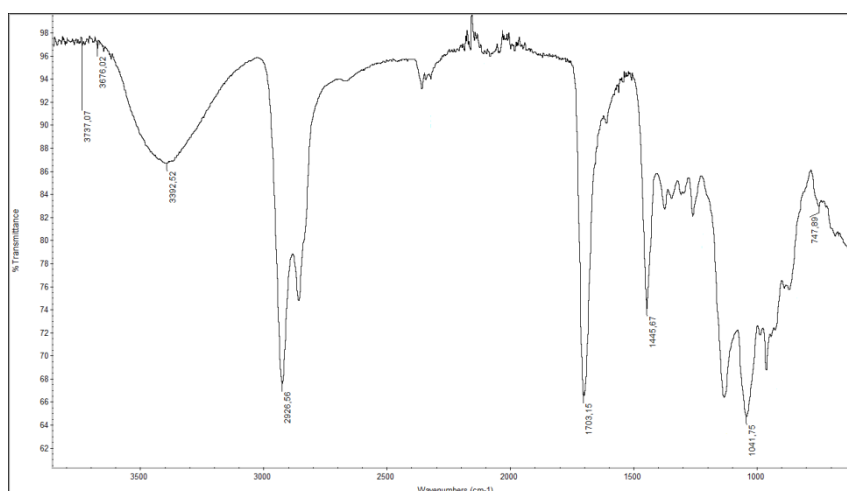


Figure 4.14: FTIR spectrum of LC-CFR4.

4.4.2. DSC thermal analysis of LC-CFR samples

In this study, as it is seen in the Figure 4.16, it is realized that the results of DSC measurements, T_g values of LC-CFR1, LC-CFR2 and LC-CFR3 samples were determined as $60\text{ }^\circ\text{C}$, $61\text{ }^\circ\text{C}$, and $68\text{ }^\circ\text{C}$, respectively. The T_g value of neat CFR was determined as $45\text{ }^\circ\text{C}$. As it seen in the Figure 4.15, T_g values of clay containing samples slightly change with the increasing clay content (wt%).

Because of the agglomeration of clay nanoparticles after 1,5 wt%, optimal clay content level was detected at the level of 1,5 wt%. It can be said that the nanocomposite of resin samples shows enhanced glass transition temperature points with addition of MMT to resin media to an optimal level. Increasing of glass transition temperature points were specified nearly %50 in comparison with neat CFR.

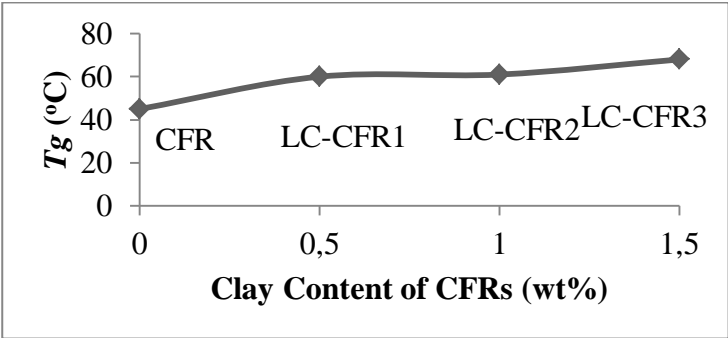


Figure 4.15: Variation of T_g (°C) for various resin clay nanocomposites with different filler contents.

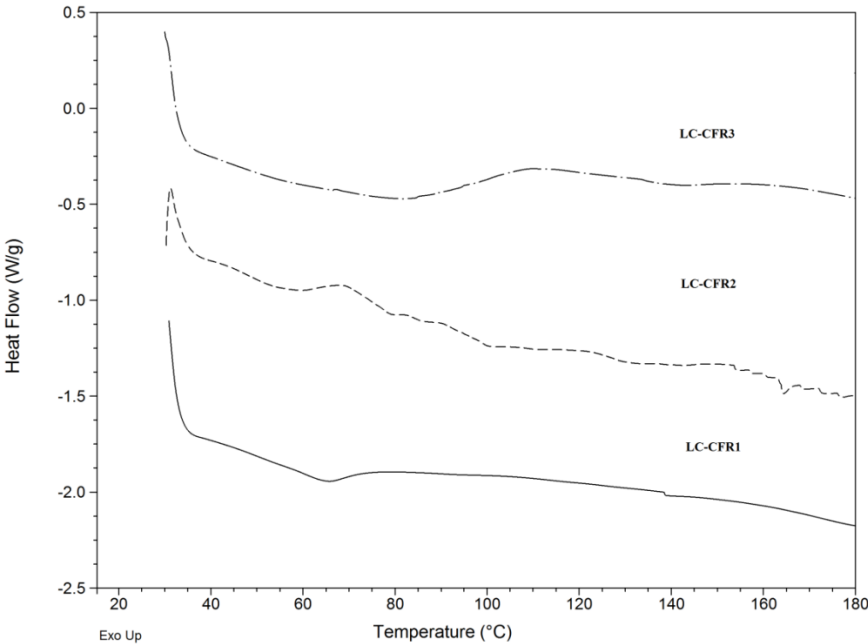


Figure 4.16: DSC thermogram of LC-CFR samples.

4.4.3. TGA thermal analysis of LC-CFR samples

Thermal decomposition behaviors of neat CFR, LC-CFR1, LC-CFR2, LC-CFR3 and LC-CFR4 were determined via TGA measurements. Degregation was carried out in a static air atmosphere until the maximum temperature of 800 °C. Onset temperature of

degradation ($^{\circ}\text{C}$), temperature at %50 residue amount and residue amount (%) at 500°C was calculated and these values are given in the Table 4.3. Also, thermograms of neat CFR, LC-CFR1, LC-CFR2, LC-CFR3 and LC-CFR4 were given in the Figure 4.17.

Table 4.3: TGA values of CFR and LC-CFRs.

Samples	Onset Temperature of Degradation($^{\circ}\text{C}$)	$T_{\%50}$ ($^{\circ}\text{C}$)	Residue (%) at 500°C
CFR	141	344	2,1
LC-CFR1	143	328	2,3
LC-CFR2	148	350	2,3
LC-CFR3	152	352	2,6
LC-CFR4	164	338	9,8

As it seen in the Figure 4.17, different stages of degradation obtained. In the first stage (until 350°C) formaldehyde was released and methylene bridges were broke. Then, the second stage of decomposition, oxidation of the network were occurred. It can be clearly seen, addition of clay to the resin media help to improve thermal resistance of neat CFR. As it seen in the table, $T_{\%50}$ ($^{\circ}\text{C}$) value of LC-CFR1 and LC-CFR4 is lower than neat CFR, agglomeration might be the reason for this.

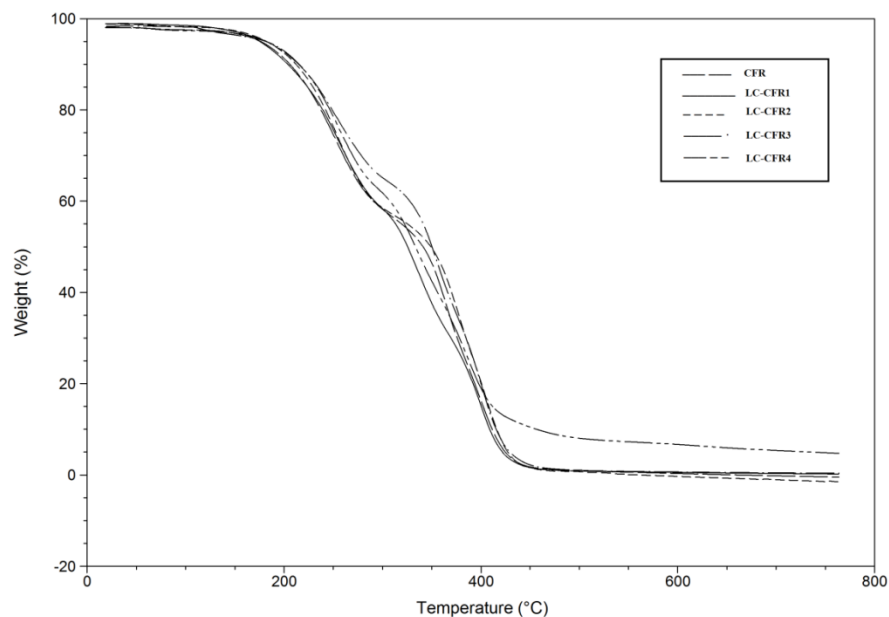


Figure 4.17: TGA thermograms of CFR and LC-CFRs.

4.4.4. XRD analysis of LC-CFR samples

By using Bragg equation, the distances between clay sheets of resin/clay nanocomposites are calculated from their XRD test results. Wavelength of radiation (λ) used was 0,7698 Å.

Bragg equation: $\lambda = 2d \sin\theta$

XRD patterns, 2θ measurements of samples was given in the Figure 4.18. The 2θ value of neat montmorillonite clay used was found at 7.3° . As it seen in the figure, 2θ values shifted lower 2θ degrees comparison with neat clay. In the Table 4.4, it can be seen the 2θ values of samples and calculated measurements of d_{001} spaces between clay sheets.

In this case the interlayer space was increased from 12.2 Å to 15.7 Å. Increase of space between layers was about from 19% to 28% for different clay containing resin/clay nanocomposites. Best results achieved for 3 wt% clay containing nanocomposite which is LC-CFR4.

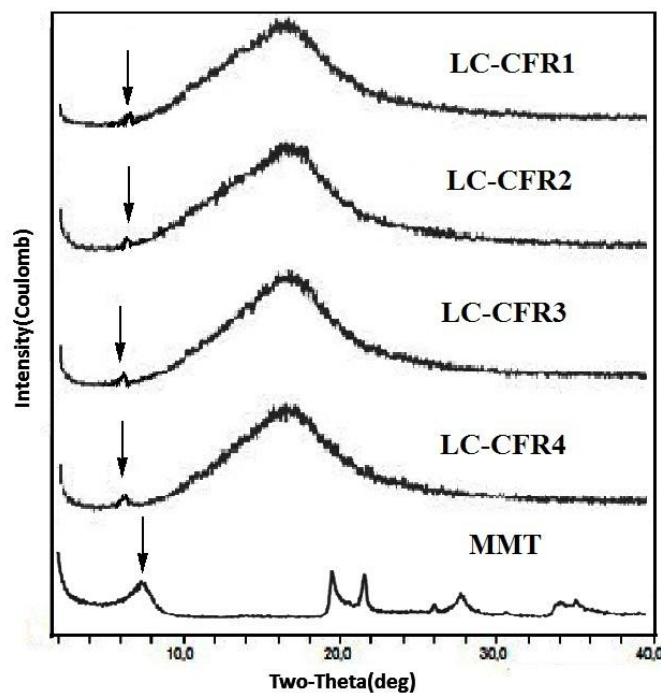


Figure 4.18: XRD patterns of LC-CFR samples.

It can be said, results indicate that the interlayer space of pristine clay was increased significantly by one step process and this results shows the intercalation of clay molecules in the resin media was successfully achieved.

Table 4.4: Interlayer spaces between clay sheets of LC-CFR samples.

Sample	Additive, wt% of clay	2 θ (°)	d ₀₀₁ (Å)
Pristine Clay	-	7.03	12.2
LC-CFR1	0.5	6.02	14.6
LC-CFR2	1	6.02	14.6
LC-CFR3	1,5	5.74	15.3
LC-CFR4	3	5.60	15.7

4.4.5. SEM analysis of LC-CFR samples

SEM analysis were done because of understanding of dispersion of clay particles in resin media and observe the intercaliation of clay layers. For conventional imaging in the SEM, specimens must be electrically conductive, at least at the surface. Because of that reason surfaces of nanocomposite samples plated with gold before examined.

SEM images of LC-CFR1, LC-CFR2, LC-CFR3 and LC-CFR4 were shown in Figure 4.19, Figure 4.20, Figure 4.21 and Figure 4.22 respectively. As it seen in figures, embedded nano clay particles can be seen on the samples surfaces. With magnification x15,000 homogeneous dispersion of clay particles can be seen. Also with magnification of x50,000 or higher, angled clay particles became visible. In addition, microvoids were observed because of the curing of by-product of water molecules released during the polymerization reaction.

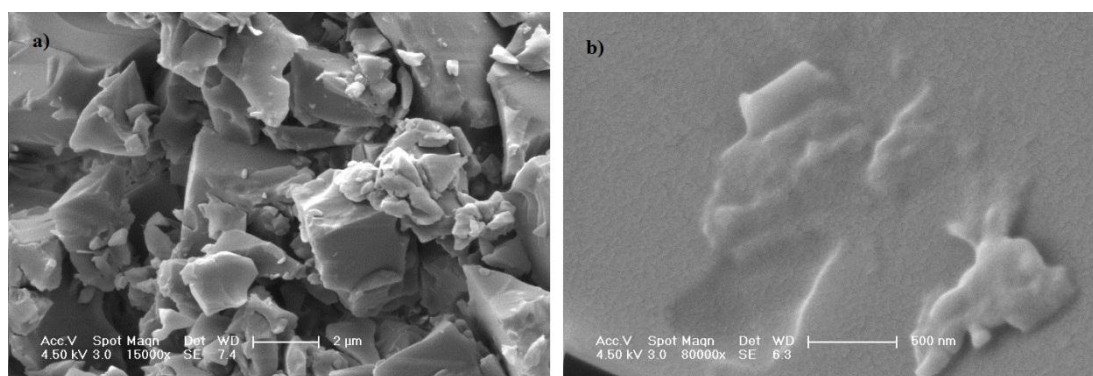


Figure 4.19: SEM images of LC-CFR1 (a; x15,000, b; x80,000).

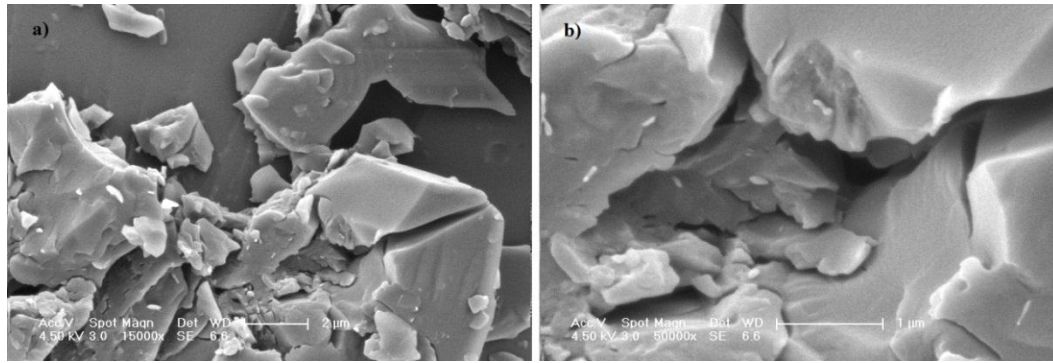


Figure 4.20: SEM images of LC-CFR2 (a; x15,000, b; x50,000).

Homogen dispersing of clay particles was not a problem for samples having clay contents of 0.5 wt%, 1 wt% and 1.5 wt%. But after having content of 1.5 wt%, as it seen in the Figure 4.22 (b), agglomeration of clay particles occurred. High surface energy of nanoparticles force them to agglomerate and to form clay tactoids. Therefore clay content higher than 1.5 wt% had the problem to disperse homogeneously. Dispersion can be improved by using techniques like high shear mixing and ultrasonication. Also modification of pristine clay may help the better dispersion of clay particles in the resin media. In this study, the amount of dispersed clay in CFR media was achieved with 1.5 wt% MMT.

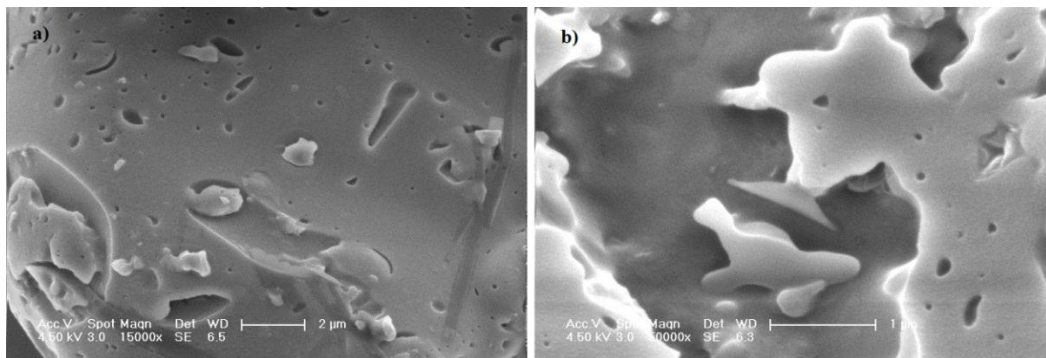


Figure 4.21: SEM images of LC-CFR3 (a; x15,000, b; x50,000).

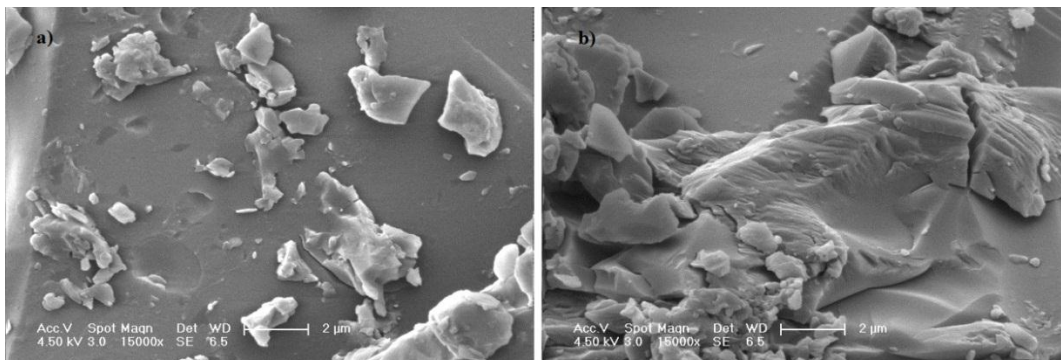


Figure 4.22: SEM images of LC-CFR4 (a; x15,000, b; x15,000).

4.5. Characterization of DA.PDMS-LC-CFR Nanocomposite Samples

4.5.1. FTIR-ATR spectroscopy of LC-CFR nanocomposite samples

The FTIR spectrum of DA.PDMS-LC-CFR1 was illustrated in Figure 4.23 and the characteristic peaks of DA.PDMS-LC-CFR1 were observed at 3382 cm^{-1} , 2926 cm^{-1} , 1698 cm^{-1} , 1445 cm^{-1} , 1043 cm^{-1} , 864 cm^{-1} and 749 cm^{-1} . These peaks respectively attributed to hydroxy methyl groups, aliphatic $-\text{CH}_2$, carbonyl $\text{C}=\text{O}$, $-\text{CH}_2$ methylene bridges, stretching of Si-O-Si of MMT and DA.PDMS, Si-CH_3 of DA.PDMS and finally deformation of Si-O-Si of MMT.

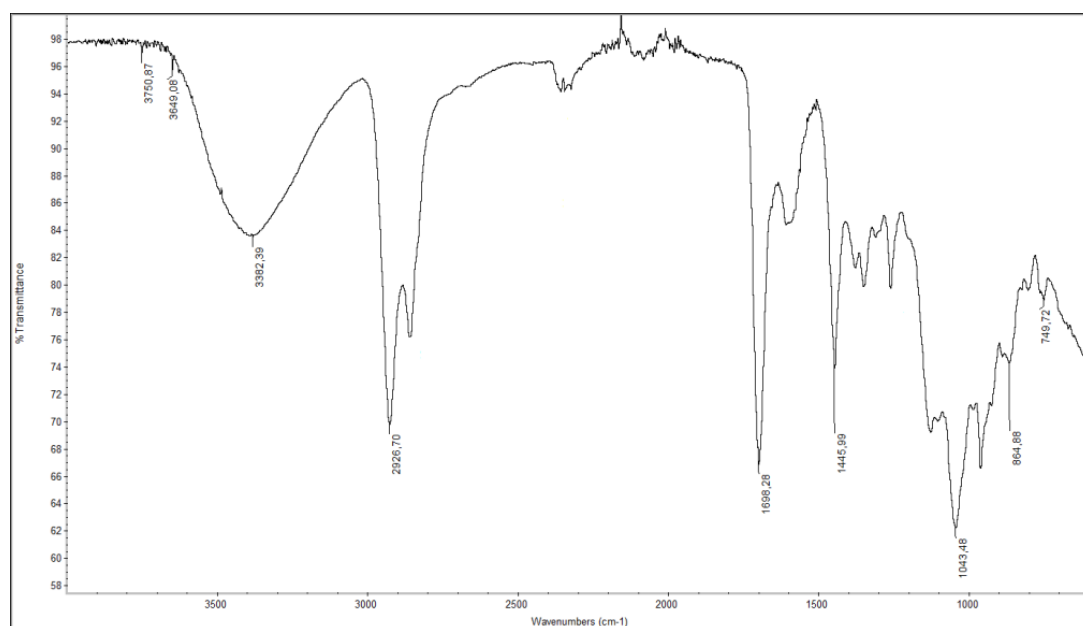


Figure 4.23: FTIR spectrum of DA.PDMS-LC-CFR1.

The FTIR spectrum of DA.PDMS-LC-CFR2 was illustrated in Figure 4.24 and the characteristic peaks of DA.PDMS-LC-CFR2 were observed at 3392 cm^{-1} , 2926 cm^{-1} , 1698 cm^{-1} , 1445 cm^{-1} , 1042 cm^{-1} , 863 cm^{-1} and 750 cm^{-1} . These peaks respectively attributed to hydroxy methyl groups, aliphatic $-\text{CH}_2$, carbonyl $\text{C}=\text{O}$, $-\text{CH}_2$ methylene bridges, stretching of Si-O-Si of MMT and DA.PDMS, Si-CH_3 of DA.PDMS and finally deformation of Si-O-Si of MMT.

The FTIR spectrum of DA.PDMS-LC-CFR3 was illustrated in Figure 4.25 and the characteristic peaks of DA.PDMS-LC-CFR3 were observed at 3392 cm^{-1} , 2926 cm^{-1} , 1698 cm^{-1} , 1445 cm^{-1} , 1044 cm^{-1} , 867 cm^{-1} and 749 cm^{-1} . These peaks respectively attributed to hydroxy methyl groups, aliphatic $-\text{CH}_2$, carbonyl $\text{C}=\text{O}$, $-\text{CH}_2$ methylene

bridges, stretching of Si-O-Si of MMT and DA.PDMS, Si-CH₃ of DA.PDMS and finally deformation of Si-O-Si of MMT.

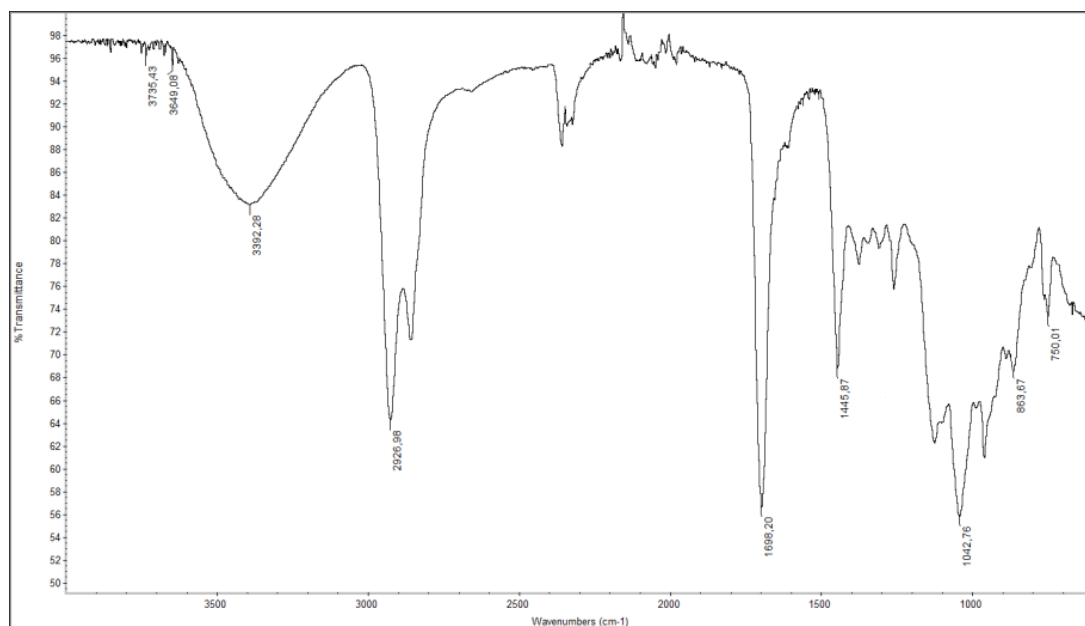


Figure 4.24: FTIR spectrum of DA.PDMS-LC-CFR2.

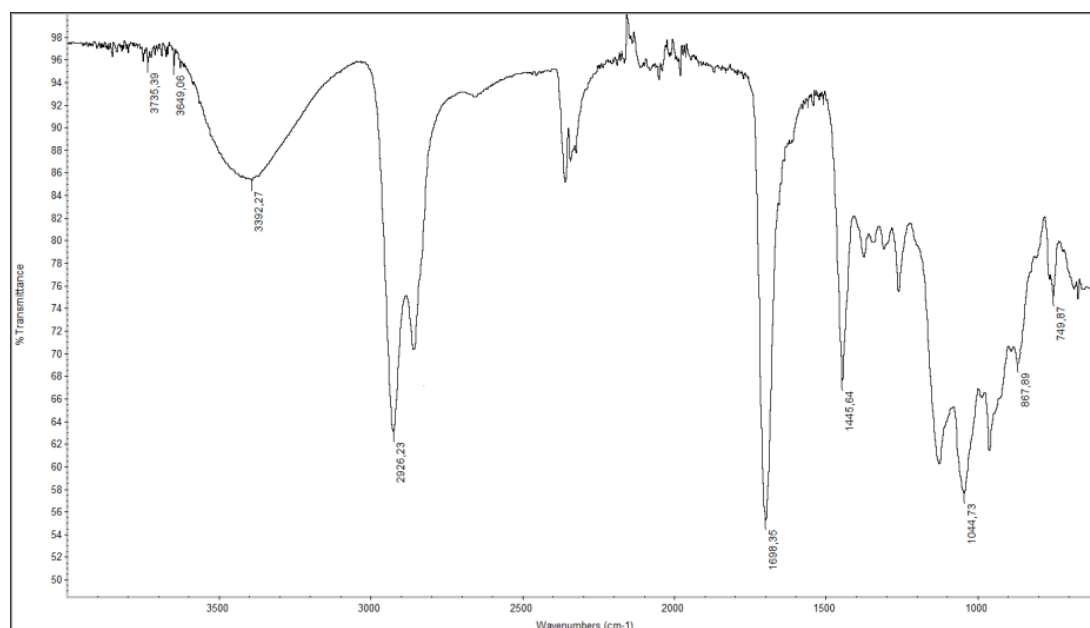


Figure 4.25: FTIR spectrum of DA.PDMS-LC-CFR3.

The FTIR spectrum of DA.PDMS-LC-CFR4 was illustrated in Figure 4.26 and the characteristic peaks of DA.PDMS-LC-CFR4 were observed at 3399 cm⁻¹, 2926 cm⁻¹, 1701 cm⁻¹, 1445 cm⁻¹, 1045 cm⁻¹, 865 cm⁻¹ and 756 cm⁻¹. These peaks respectively attributed to hydroxy methyl groups, aliphatic -CH₂, carbonyl C=O, -CH₂ methylene

bridges, stretching of Si-O-Si of MMT and DA.PDMS, Si-CH₃ of DA.PDMS and finally deformation of Si-O-Si of MMT.

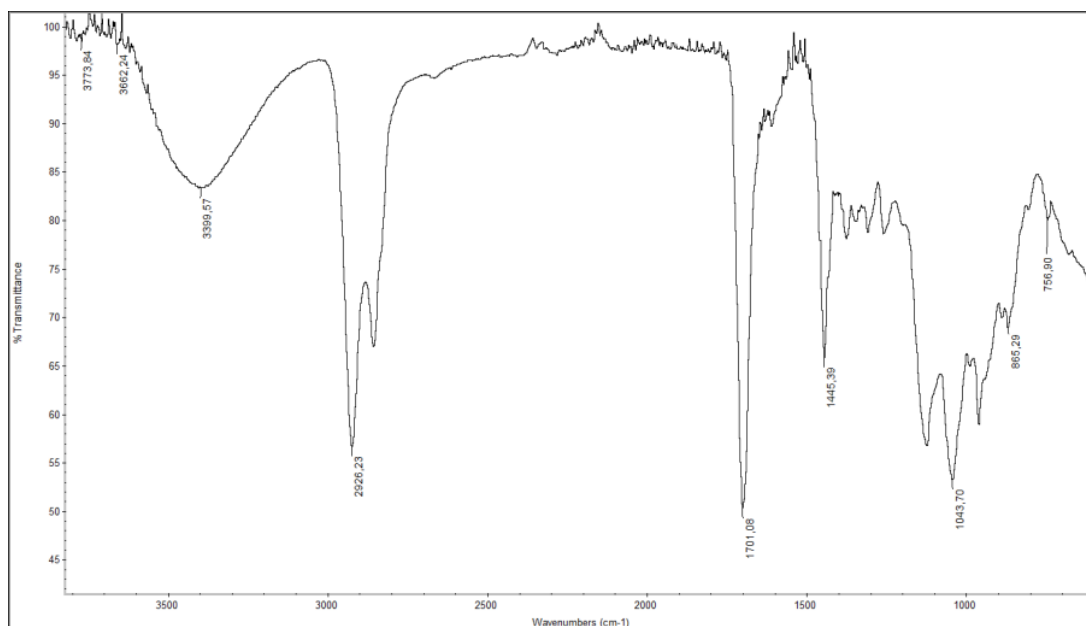


Figure 4.26: FTIR spectrum of DA.PDMS-LC-CFR4.

4.5.2. DSC thermal analysis of DA.PDMS-LC-CFR samples

In this study, as it is seen in the Figure 4.28, it is realized that the results of DSC measurements, T_g values of DA.PDMS-LC-CFR1, DA.PDMS-LC-CFR2, DA.PDMS-LC-CFR3 and DA.PDMS-LC-CFR4 samples were determined as 119 °C, 113 °C, 117 °C and 122 °C, respectively. The T_g value of DA.PDMS-CFR was determined as 68 °C. As it seen in the Figure 4.27, T_g values of clay containing samples slightly change with the increasing clay content (wt%).

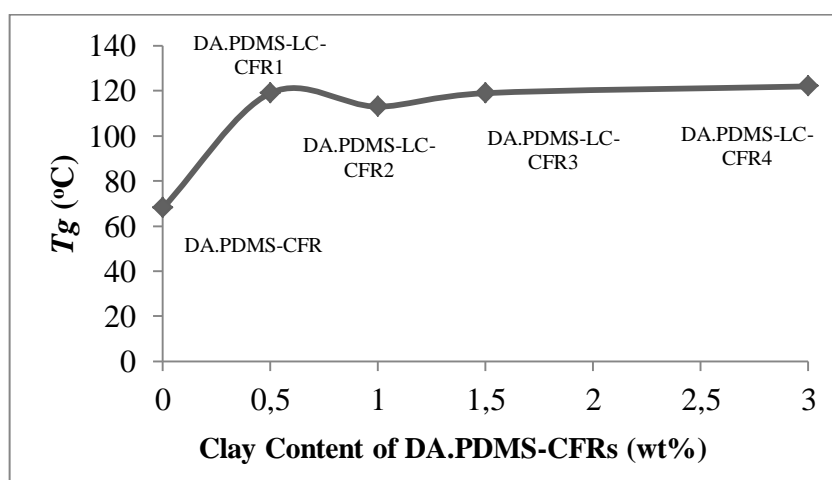


Figure 4.27: Variation of T_g (°C) for various resin clay nanocomposites with different filler contents.

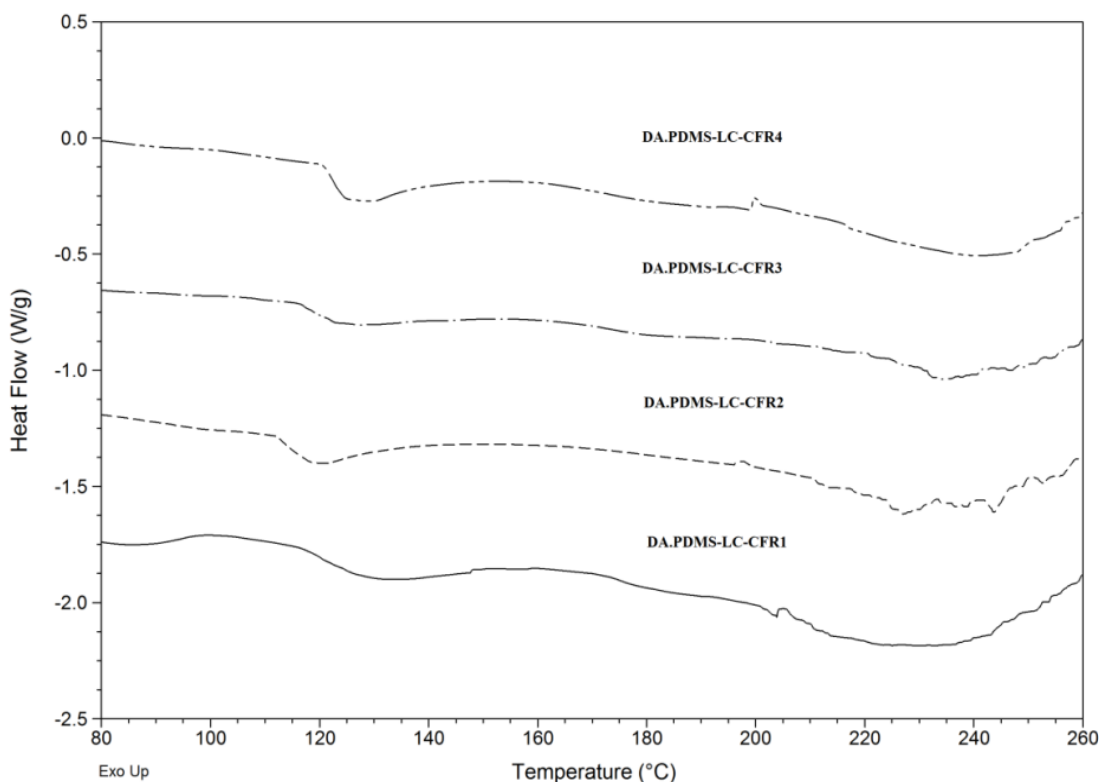


Figure 4.28: DSC thermogram of DA.PDMS-LC-CFR samples.

Because of the agglomeration of clay nanoparticles after 1,5 wt%, optimal clay content level was detected at the level of 1,5 wt%. It can be said that the nanocomposite of resin samples shows enhanced glass transition temperature points with addition of MMT to resin media to an optimal level. Increasing of glass transition temperature points were specified nearly %78 in comparison with neat DA.PDMS-CFR.

4.5.3. TGA thermal analysis of DA.PDMS-LC-CFR samples

Thermal decomposition behaviors of neat DA.PDMS-CFR, DA.PDMS-LC-CFR1, DA.PDMS-LC-CFR2, DA.PDMS-LC-CFR3 and DA.PDMS-LC-CFR4 were determined via TGA measurements. Degregation was carried out in a static air atmosphere until the maximum temperature of 800 °C. Onset temperature of degradation (°C), temperature at %50 residue amount and residue amount (%) at 500 °C was calculated and these values are given in the Table 4.5. Also, thermograms of neat DA.PDMS-CFR, DA.PDMS-LC-CFR1, DA.PDMS-LC-CFR2, DA.PDMS-LC-CFR3 and DA.PDMS-LC-CFR4 were given in the Figure 4.29.

As it seen in the Figure 4.29, different stages of degradation obtained. In the first stage (until 350 °C) formaldehyde was released and methylene bridges were broke. Then, the second stage of decomposition, oxidation of the network were occurred. It can be clearly seen, addition of clay to the resin media help to improve thermal resistance of neat DA.PDMS-CFR. As it seen in the table, % residue amount at 500 °C value of DA.PDMS-LC-CFR4 is lower than neat DA.PDMS-CFR, agglomeration might be the reason for this.

Table 4.5: TGA values of DA.PDMS-CFR and DA.PDMS-LC-CFRs.

Sample	Onset Temperature of Degradation(°C)	$T_{%50}$ (°C)	Residue (%) at 500 (°C)
DA.PDMS-CFR	144	336	2,4
DA.PDMS-LC-CFR1	151	337	2,4
DA.PDMS-LC-CFR2	156	336	2,1
DA.PDMS-LC-CFR3	166	352	2,2
DA.PDMS-LC-CFR4	150	336	2,5

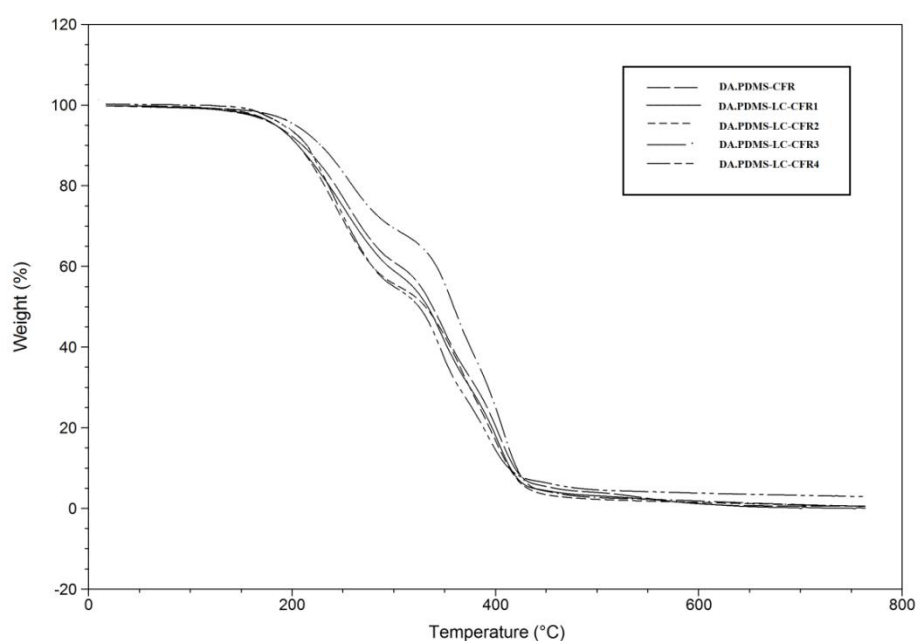


Figure 4.29: TGA thermograms of DA.PDMS-CFR and DA.PDMS-LC-CFRs.

4.5.4. XRD analysis of DA.PDMS-LC-CFR samples

By using Bragg equation, the distances between clay sheets of resin/clay nanocomposites are calculated from their XRD test results. Wavelength of radiation (λ) used was 0,7698 Å.

Bragg equation: $\lambda = 2d \sin\theta$

XRD patterns, 2θ measurements of samples was given in the Figure 4.30. The 2θ value of neat montmorillonite clay used was found at 7.3° . As it seen in the figure, 2θ values shifted lower 2θ degrees comparison with neat clay. In the Table 4.6, it can be seen the 2θ values of samples and calculated measurements of d_{001} spaces between clay sheets.

In this case the interlayer space was increased from 12.2 Å to 14.9 Å. Increase of space between layers was about from 7% to 22% for different clay containing resin/clay nanocomposites. Best results achieved for 3 wt% clay containing nanocomposite which is DA.PDMS-LC-CFR4.

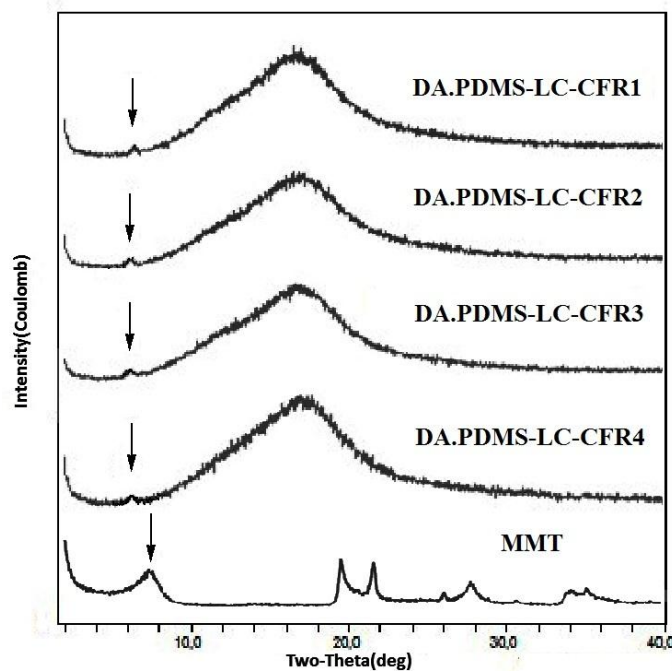


Figure 4.30: XRD patterns of DA.PDMS-LC-CFR samples.

It can be said, results indicate that the interlayer space of pristine clay was increased significantly by one step process and this results shows the intercalation of clay molecules in the resin media was successfully achieved.

Table 4.6: Interlayer spaces between clay sheets of DA.PDMS-LC-CFR samples.

Sample	Additive, wt% of clay	2 θ (°)	d ₀₀₁ (Å)
Pristine Clay	100	7.03	12.2
DA.PDMS-LC-CFR1	0.5	6.76	13.1
DA.PDMS-LC-CFR2	1	6.26	14.1
DA.PDMS-LC-CFR3	1,5	6.10	14.5
DA.PDMS-LC-CFR4	3	5.90	14.9

4.5.5. SEM analysis of DA.PDMS-LC-CFR samples

SEM analysis were done because of understanding of dispersion of clay particles in resin media and observe the intercaliation of clay layers. For conventional imaging in the SEM, specimens must be electrically conductive, at least at the surface. Because of that reason surfaces of nanocomposite samples plated with gold before examined.

SEM images of DA.PDMS-LC-CFR1, DA.PDMS-LC-CFR2, DA.PDMS-LC-CFR3 and DA.PDMS-LC-CFR4 were shown in Figure 4.31, Figure 4.32, Figure 4.33 and Figure 4.34 respectively. As it seen in figures, embedded nano clay particles can be seen on the samples surfaces. With magnification x15,000 homogeneous dispersion of clay particles can be seen. Also with magnification of x50,000 or higher, angled clay particles became visible. In addition, microvoids were observed because of the curing of by-product of water molecules released during the polymerization reaction.

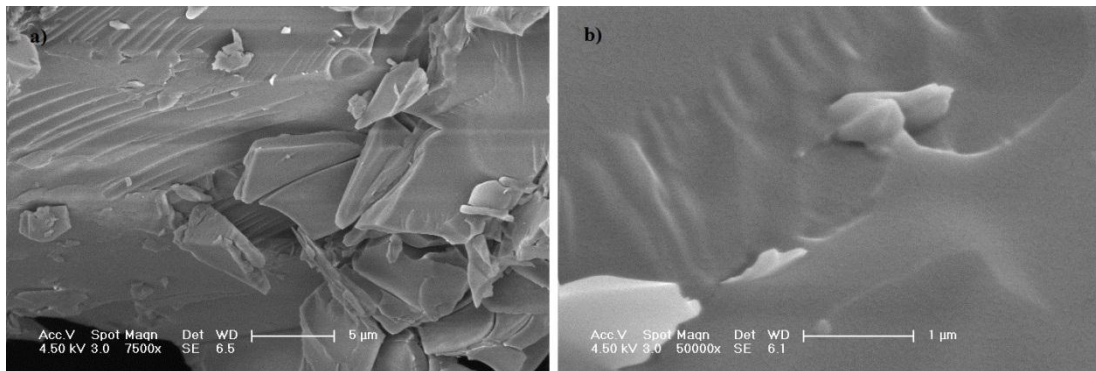


Figure 4.31: SEM images of DA.PDMS-LC-CFR1 (a; x7,500, b; x50,000).

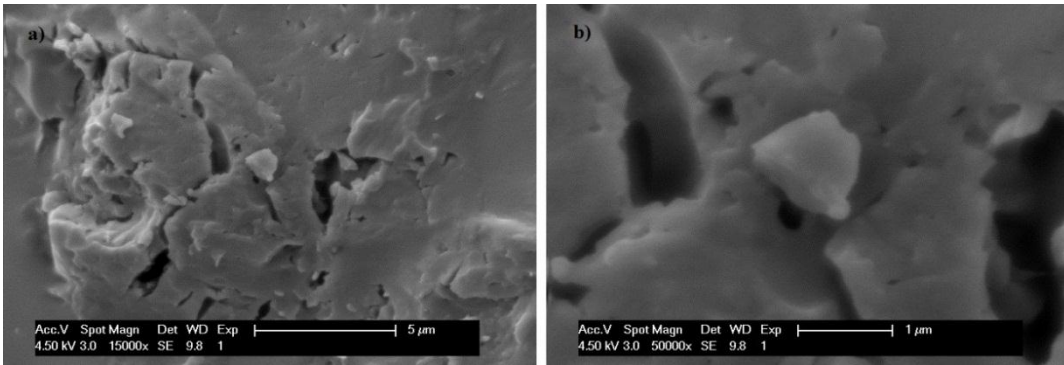


Figure 4.32: SEM images of DA.PDMS-LC-CFR2 (a; x15,000, b; x50,000).

Homogen dispersing of clay particles was not a problem for samples having clay contents of 0.5 wt%, 1 wt% and 1.5 wt%. But after having content of 1.5 wt %, as it seen in the Figure 4.34 (b), agglomeration of clay particles occurred. High surface energy of nanoparticles force them to agglomerate and to form clay tactoids. Therefore clay content higher than 1.5 wt% had the problem to disperse homogeneously. Dispersion can be improved by using techniques like high shear mixing and ultrasonication. Also modification of pristine clay may help the better dispersion of clay particles in the resin media. In this study, the amount of dispersed clay in DA.PDMS-CFR media was achieved with 1.5 wt% MMT.

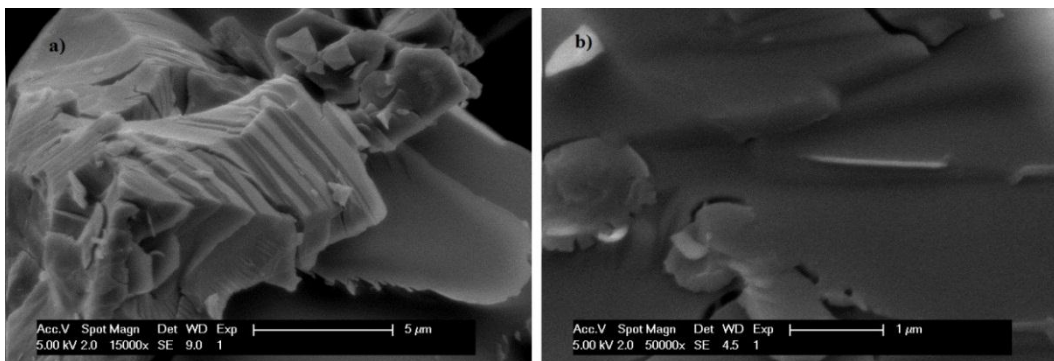


Figure 4.33: SEM images of DA.PDMS-LC-CFR3 (a; x15,000, b; x50,000).

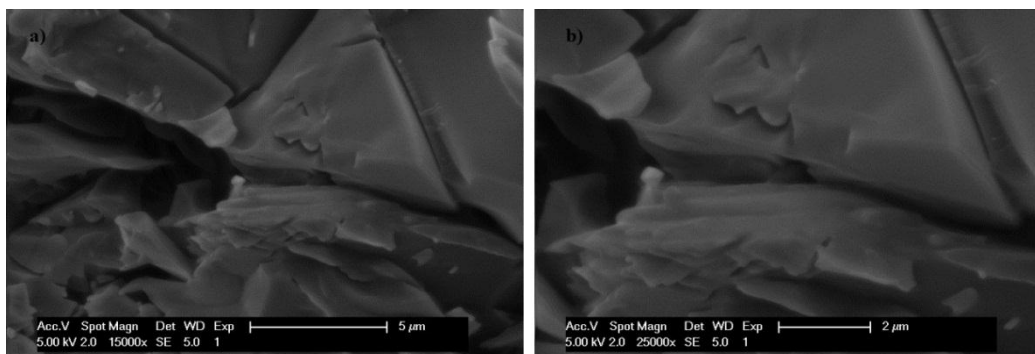


Figure 4.34: SEM images of DA.PDMS-LC-CFR4 (a; x15,000, b; x25,000).

5. CONCLUSION

FTIR and ¹H-NMR results of final samples indicates that copolymers of polydimethylsiloxane cyclohexanone formaldehyde and nanocomposites forms of resin samples were successfully synthesized with one step process. When looking at the thermal analysis results, the glass transition temperatures and heat resistance levels of final samples were clearly shown to be increased by the addition of PDMS and MMT clay to the resin media. Increased levels were determined by using these results and they were used in explaining the conditions in detail. In order to determine the basal spaces of MMT clay in resin media XRD analysis were used and the results show that the interlayer space of pristine clay was increased significantly and these results show that the intercalation of clay molecules in the resin media was successfully achieved. Also homogeneous dispersion of clay can be seen in SEM images until the weight percentage of clay wt 1.5 %, and above this percentage clay tactoids can be seen due to the agglomeration of clay nanoparticles. It can be said determining factor of clay content is agglomeration which is about wt 1.5% content of clay in the resin media.

This study showed that as a ketonic resin cyclohexanone formaldehyde can be synthesized as a form of nanocomposite with direct addition of clay nanoparticles into the resin media, also all known resin/layered silicate nanocomposites, such as epoxy or phenolic resins, can be reacted to become nanocomposites with this one step process in situ modification.

REFERENCES

- [1] **Giannelis, E. P.** (1996). Polymer layered silicate nanocomposites, *Advanced Materials*, **8**, pp. 29.
- [2] **Blumstein, A.** (1965). Polymerization of adsorbed monolayers. II. Thermal degradation of the inserted polymer, *Journal of Polymer Science Part A*, **3** pp. 2665.
- [3] **Kojima, Y., Usuki, A., Kawasumi, M., Okada, A., Karauchi T. and Kamigaito, O.** (1993). Sorption of water in nylon 6-clay hybrid, *J. Polym. Sc. Part, A*, **49**, pp. 1259.
- [4] **Giannelis, E. P.** (1992). A new strategy for synthesizing polymer-ceramic nanocomposites, *JOM*, **44**, pp. 28.
- [5] **Gleiter, H.** (1992). Nanostructured Materials, *Advanced Materials*, **4**, 474.
- [6] **Novak, B. M.** (1993). Hybrid Nanocomposite Materials between inorganic glasses and organic polymers, *Advanced Materials*, **5**, 422.
- [7] **Gelfer, M., Burger, C., Fadeev, A., Sics, I., Chu, B. and Hsiao, B. S.** (2004). Thermally induced phase transitions and morphological changes in organoclays, *NCBI*, **20**, pp. 3746.
- [8] **Biswas, M. and Ray, S. S.** (2001). Recent progress in synthesis and evaluation of polymer-montmorillonite nanocomposites in New Polymerization Techniques and Synthetic Methodologies, *Advances in Polymer Science*, **155**, pp. 167–221, Springer, Berlin, Germany.
- [9] **Giannelis, E. P., Krislmamoorti, R. and Manias, E.** (1999). Polymer-Silicate Nanocomposites: Model Systems for Confined Polymers and Polymer Brushes, *Advances in Polymer Science*, **138**, 108.
- [10] **Vaia, H. A., Price, G., Ruth, P. N., Nguyen, H. T. and Lichtentmn, J.** (1999). Polymer/layered silicate nanocomposites as high performance ablative materials, *Applied Clay Science*, **15**, 67.
- [11] **Vaia, K.A., Ishii H. and Giannelis, E. P.** (1993). Synthesis and properties of two-dimensional nanostructures by direct intercalation of polymer melts in layered silicates, *Chemistry of Materials*, **5**, 1694.
- [12] **Bharadwaj, R. K.** (2001). Modeling the barrier properties of polymer-layered silicate nanocomposites, *Macromolecules*, **34**, 9189.
- [13] **Xu R., Manias E., Snyder A. J. and Runt J.** (2001). New biomedical poly (urethane urea)-layered silicate nanocomposites, *Macromolecules*, **34**, 337.
- [14] **Yano K., Usuki A., Okada A., Kurauchi, T. and Kamigaito, O.** (1993). Synthesis and properties of polyimide–clay hybrid, *Journal of Polymer Science, Part. A: Polymer Chemistry*, **31**, 2493.

- [15] **Gilman, J. W.** (1999). Flammability and thermal stability studies of polymer layered-silicate (clay) nanocomposite, *Applied Clay Science*, **15**, 31.
- [16] **Gilman, J. W., Jackson, C. L., Morgan, A. B., Harris, Jr. R., Manias, E., Giannelis, E. P., Wuthenow, M., Hilton D. and Phillips S. H.** (2000). Flammability Properties of Polymer–Layered-Silicate Nanocomposites. Polypropylene and Polystyrene Nanocomposites, *Chemistry of Materials*, **12**, 1866.
- [17] **Liu, T., Tjiu W. C., He, C., Na, S.S. and Chung, T.S.** (2004). A processing-induced clay dispersion and its effect on the structure and properties of polyamide, *Polymer International*, **653**, 392.
- [18] **Lee, A. and Lichtenhan, J.D.** (1999). Thermal and viscoelastic property of epoxy–clay and hybrid inorganic–organic epoxy nanocomposites, *J. Appl. Polym. Sc.*, **73**, 1993-2001,
- [19] **Kim, G.M., Lee, D.H., Hoffmann, B., Kressler, J. and Stoppelmann, G.** (2001). Influence of nanofillers on the deformation process in layered silicate/polyamide-12 nanocomposites, *Polymer*, **42**, 1095.
- [20] **Hussain, F., Hojjati, M. Okamoto, M., Gorga, R. E.** (2006). Review article: Polymer-matrix Nanocomposites, Processing, Manufacturing, and Application: An Overview, *Journal of Composite Materials*, **40**, 1511.
- [21] **Gorga, R. E. and Cohen, R. E.** (2004). Toughness enhancements in poly(methyl methacrylate) by addition of oriented multiwall carbon nanotubes, *Journal of Polymer Science Part B: Polymer Physics*, **42**, 2690.
- [22] **Ray, S. S., Yamada, K., Okamoto, M., Fujimoto Y., Ogami, A., and Ueda, K.** (2003). New polylactide/layered silicate nanocomposites. 5. Designing of materials with desired properties, *Polymer*, **44**, 6633.
- [23] **Halpern, Y., Mott, D.M., and Niswander, R.H.** (1984). Fire retardancy of thermoplastic materials by intumescence, *Ind. Eng. Chem. Prod. Res.Dev.*, **23**, 233.
- [24] **Clio, J. W., and Paul, D. R.** (2001). Nylon 6 nanocomposites by melt compounding, *Polymer*, **42**, 1083.
- [25] **Thostenson, R., Li, C., and Cuioli, T.** (2005) Nanocomposites in context, *Composites Science and Technology*, **65**, 491.
- [26] **Schmidt, D., Shall, D., and Giannelis, E.P.** (2002). New advances in polymer/layered silicate nanocomposites, *Solid State and Materials Science*, **6**, 205.
- [27] **Roylance, D.** (2000). Introduction to composite materials, *Dep. of Mat. Science & Eng., Massachusetts Institute of Technology*.
- [28] **Pandey, P., C.** (2004). Composite Materials Web based course, *Dept. of Civil Eng., IISc Bangalore*.
- [29] **Kızılcan, N., Akar, A.** (2005). Modification of Cyclohexanone–Formaldehyde Resins with Silicone Tegomers, *Journal of Applied Polymer Science*, **98**, 97–101.

- [30] **Stoye, D. and Freitag, W.** (1996). Resins for Coatings: Chemistry, Properties and Applications, *Hasnser/Gardner Publications Inc.*, pp.1.
- [31] **Url-1**<<http://composite.about.com/od/aboutcompositesplastics/a/Thermoplastic-Vs-Thermoset-Resins.htm>>, date retrieved 28.11.2012.
- [32] **Kittel, H.** (1971). Lehrbuch der Lacke und Beschichtungen, Vol. I/I., *Verlag wa Colomb*, Stuttgart,Berlin, pp. 390.
- [33] **Gerhartz, W. and Schulz, G.** (1976). Ullmanns Encyclopadie der technischen Chemie, 4th ed., Vol. 12. Verlag Chemie, Weinheim, pp. 547-555.
- [34] **Stoye, D. and Freitag, W.** (1996). Resins for Coatings: Chemistry, Properties and Applications, *Hasnser/Gardner Publications Inc.*, pp.159.
- [35] **Scheiber, J.** (1961). Chemie und Technologie der kiinstlichen Harze, Vol. 1. *Wissenschaftl Verlagsges*, Stuttgart, pp. 164-165.
- [36] **Wagner, H. and Sarx, H. F.** (1971). Lackkunsthharze. 5th ed. *Hanser*, Munchen, pp. 84-85.
- [37] **Stoye, D. and Freitag, W.** (1996). Resins for Coatings: Chemistry, Properties and Applications, *Hasnser/Gardner Publications Inc.*, pp. 160.
- [38] **Stoye, D. and Freitag, W.** (1996). Resins for Coatings: Chemistry, Properties and Applications, *Hasnser/Gardner Publications Inc.*, pp. 161-162.
- [39] **Luttgen, C.** (1959). Die Technologie der Klebstoffe, Part 1, 2nd ed., *Pansegrau*, Berlin, pp. 212 .
- [40] **Engelhardt, F. and Wollner, J.** (1963). *Brennst. Chem.* 44-52.
- [41] **Houben, H. and Weyl, T.** (1963.). Methoden der organischen Chemie, 4th Ed., Vol. XIV/2. *Thieme*, Stuttgart, pp. 416.
- [42] **Buszewski, B. and Suprynowicz Z.** (1980). *Chem. Zvesti*, **42** pp. 835-840.
- [43] **Katti, D. and Patil, S.** (1993). *Paintindia* (1993), **9**, pp. 15-20.
- [44] **Stoye, D. and Freitag, W.** (1996). Resins for Coatings: Chemistry, Properties and Applications, *Hasnser/Gardner Publications Inc.*, pp. 163.
- [45] **Freitag, W.** (1993). Ullmanns Encyclopedia of Industrial Chemistry, 55th Ed., Vol. 23. *VCH*, Weinheim, pp. 99-105.
- [46] **Stoye, D. and Freitag, W.** (1996). Resins for Coatings: Chemistry, Properties and Applications, *Hasnser/Gardner Publications Inc.*, pp. 164.
- [47] **Nakane, S., Yoshida, A. and Takahashi, S.** (1987-1988). *Jpn. Kokai Tokkyo Koho JP Patent*, 62,179,847 and *Chem. Abstr.Ser.*, 108,959,022.
- [48] **Jaroslov, C., Karel, J., Stanislav, S., Milan, S. and Jan, D.** (1989) *Czech. CS Patent*, 254,841 and *Chem. Abstr.Ser.*, 111,215,499.
- [49] **Uyanik, N., Kizilcan, N. And Akar, A.** (1997). ABA-Type Block Copolymers Containing Poly (dimethylsiloxane) and Ketonic Resins, *Journal of Applied Polymer Science*, **67**, 643–648.
- [50] **Oriakhi, C. O.** (1996). Post Graduate Thesis, Studies on the Synthesis and Characterization of Polymer-Containing Nanocomposite Materials, *Oregon State University*.

- [51] **Andersen, P.** (2010). Polymer Nanocomposites Handbook, *Taylor and Francis Group*, pp.97.
- [52] **Giannelis, E. P.** (1996). Polymer layered silicate nanocomposites, *Adv. Mater.*, **8**, 29.
- [53] **Lan, T. and Pinnavaia, T. J.** (1994). Clay-reinforced epoxy nanocomposites, *Chem. Mater.*, **6**, 2216.
- [54] **Shi, H., Lan, T., and Pinnavaia, T. J.** (1996). Interfacial effects on the reinforcement properties of polymer-organoclay nanocomposites, *Chem. Mater.*, **8**, 1584.
- [55] **Wang, Z. and Pinnavaia, T. J.** (1998). Nanolayer reinforcement of elastomeric polyurethane, *Chem. Mater.*, **10**, 3769.
- [56] **Yao, K.J.** (2001). Polymer/layered clay nanocomposites: 2 polyurethane nanocomposites, *Polymer*, **43**, 2981.
- [57] **Lunsford, J.** (1973). ESR of absorbed oxygen species, *Catalysis Reviews*, **8**, pp. 135-141.
- [58] **Kent, G. M., Memory, J. M., Gilber, R. D. and Fomes, R. E.** (1983). Variation in radical decay rates in epoxy as a function of crosslink density, *J. App. Polym. Sci.*, **28**, pp. 3301-3307.
- [59] **Schmidt, H. J.** (1985). Non-Cryst. Solids, New type of noncrystalline solids between inorganic and organic materials, **73**, 681–691.
- [60] **Novak, B. M.** (1993). Hybrid Nanocomposite Materials between inorganic glasses and organic polymers, *Adv. Mater*, **5**, 422–433.
- [61] **Mark, J. E.** (1996). Ceramic-reinforced polymers and polymer-modified ceramics, *Polym. Eng. Sci.*, **36**, 2905–2920.
- [62] **LeBaron, P. C., Wang, Z, and Pinnavaia, T. J.** (1999). Polymer-layered silicate nanocomposites: an overview, *Appl. Clay Sci.*, **15**, 11–29.
- [63] **Giannelis, E. P.** (1996). You have free access to this content Polymer Layered Silicate Nanocomposites, *Adv. Mater*, **8**, 29–35.
- [64] **Gilman J. W.** (1999). Flammability and thermal stability studies of polymer layered-silicate (clay) nanocomposites, *Appl. Clay Sci*, **15**, 31–49.
- [65] **Kojima, Y., Usuki, A., Kawasumi, M., Okada, A., Fukushima, Y., Kurauchi, T. and Kamigaito, O.** (1993). Mechanical properties of nylon 6-clay hybrid, *Journal of Material Research*, **8**, 1185–1189.
- [66] **Okada, A., Kawasumi, M., Usuki, A., Kojima, Y., Kurauchi, T. and Kamigaito, O.** (1990). Polymer based molecular composites, *MRS Symposium Proceedings*, Pittsburgh, **171**, 45–50.
- [67] **Jones, T. R.** (1983). The properties and uses of clays which swell in organic solvents, *Clay Minerals*, **18**, 399.
- [68] **Kaynak, C., Nakas, G. I. Isitman, N. A.** (2009). Mechanical properties, flammability and char morphology of epoxy resin/ montmorillonite nanocomposites, *Applied Clay Science*, **46**, 319–324.

- [69] **Dai, C., Li, P., Yeh, J.** (2008). Comparative studies for the effect of intercalating agent on the physical properties of epoxy resin-clay based nanocomposite materials, *European Polymer Journal*, **44**, 2439–2447.
- [70] **Guo, B., Jia, D., Cai, C.** (2004). Effects of organo-montmorillonite dispersion on thermal stability of epoxy resin nanocomposites, *European Polymer Journal*, **40**, 1743–1748.
- [71] **Garea, S. A., Nicolescu, A., Deleanu, C. and Iovu, H.** (2010). New Nanocomposites Based on Epoxy Resins Reinforced with Modified Montmorillonite, *International Journal of Polymer Anal. Charact.*, **15**, 497–508.
- [72] **Byun, H. B., Choi, M. H., and Chung, I. J.** (2001). Synthesis and Characterization of Resol Type Phenolic Resin/Layered Silicate Nanocomposites *Chem. Mater.* **13**, 4221-4226.
- [73] **Usuki, A., Mizutani, T., Fukushima, Y., Fujimoto, M., Fukomori, K., Kojima, Y., Sato, N., Kurauchi, T. and Kamikaito, O.** (1989). U.S. Patent 4,889,885.
- [74] **Choi, M. H., Chung, I. J.** (2000). Morphology and Curing Behaviors of Phenolic Resin-Layered Silicate Nanocomposites Prepared by Melt Intercalation, *Chem. Mater.*, **12**, 2977.
- [75] **Choi, M. H.** (2000). Ph.D. Thesis, *KAIST*, Korea.
- [76] **Özkaraman, G. and Kızılcan, N.** (2012-in press). In Situ Preparation of Resol/Clay Nanocomposites, *Pigment & Resin Technology*
- [77] **Kızılcan, N. and Akar, A.** (1996). Modification of Acetophenone-Formaldehyde and Cyclohexanone-Formaldehyde Resins, *Journal of Applied Polymer Science*, **60**, 465-476.
- [78] **Lei, H., Du, G., Pizzi, A. and Celzard A.** (2008). Influence of nanoclay on urea-formaldehyde resins for wood adhesives and its model, *J. Appl. Polym. Sci.*, **109**, 2442-2451.
- [79] **Ates, E., Uyanık, N. and Kızılcan, N.** (2012-in press). Preparation of urea formaldehyde resin/layered silicate nanocomposites, *Pigment & Resin Technology*.
- [80] **Alexandre, M., and Dubois, P.** (2000). Polymer-layered silicate nanocomposites: preparation, properties and uses of a new class of materials, *Materials Science and Engineering*, **28**, 1-63.
- [81] **Ray, S. S.** (2003). Masami Okamoto, Polymer/layered silicate nanocomposites: a review from preparation to processing, *Prog. Polym. Sci.*, **28** 1539–1641.
- [82] **Alexandre, M. And Dubois, P.** (2000). Polymer-layered silicate nanocomposites: preparation, properties and uses of a new class of materials, *Materials Science and Engineering*, **28**, 1-63.
- [83] **Fu, X. and Qutubuddin, S.** (2002). Nano-Surface Chemistry, *Marcel Dekker, Inc.*, Ch. 17, pp.3-4.

- [84] **Fu, X. and Qutubuddin, S.** (2002). Nano-Surface Chemistry, *Marcel Dekker, Inc.*, Ch. 17, pp.2.
- [85] **Kim, K. J. and White, J. L.** (2010). Polymer Nanocomposites Handbook, *Taylor and Francis Group, LLC.* Ch. 4 pp.46.
- [86] **Kızılcan, N., Galioglu, O. And Akar, A.** (1993). Modified cyclohexanone–formaldehyde and acetophenone–formaldehyde resins, *J Appl. Polym Sci*, **50**, 577.
- [87] **Tilichenko, M. N. and Zykova, L. V.** (1952). *J Appl Chem. USSR*, **25**, 62
- [88] **Kızılcan, N. and Akar, A.** (1999). In situ modified reactive cyclohexanone–formaldehyde resins, *Die Angewandte Makromolekulare Chemie*, **266** 1–6.
- [89] **Kizilcan, N., Hocaoglu, B. and Ustamehmetoglu, B.** (2011). Polymerization of cyclohexanone formaldehyde resin modified with carbazole-9-carbonyl chloride, *Pigment & Resin Technology*, **40**, 143–153.
- [90] **Çanak, T. Ç., Kızılcan, N. and Serhatlı, İ. E.** (2011). Synthesis of Cyclohexanone Formaldehyde Resin-Methylmethacrylate Block-Graft Copolymers via ATRP, *Journal of Applied Polymer Science*, **123**, 2628–2635.
- [91] **Holy, N., Fowler, R., Burnett, E. and Lorenz, R.** (1979). *Tetrahedron*, **35**, 613.
- [92] **Xie, W., Xie, R., Pan, W., Hunter, D., Koene, B., Tan, L. and Vaia, R.** (2002). Thermal Stability of Quaternary Phosphonium Modified Montmorillonites, *Chem. Mater.*, **14**, 4837-4845.
- [93] **Madejova, J.** (2003). FTIR techniques in clay mineral studies, *Vibrational Spectroscopy*, **31**, 1–10.
- [94] **Xi, Y., Ding, Z., He H. and Frost, R. L.** (2005). Infrared spectroscopy of organoclays synthesized with the surfactant octadecyltrimethylammonium bromide, *Spectrochimica Acta Part A: Molecular and Biomolecular Spectroscopy*, **61**, 515-25.

CURRICULUM VITAE

Name Surname: Mehmet MERMUTLU

Place and Date of Birth: 06.09.1987 - Eskişehir

Address: Bahçelievler Mah. Ferit Selim Paşa Cad. No: 99/8 Bahçelievler/İstanbul

E-Mail: mehmetmermutlu@gmail.com

B.Sc.: Eskişehir Osmangazi University - Chemistry

PRESENTATIONS ON THE THESIS

- **Mermutlu M.,** and Kızılcan N., 2012: In Situ Preparation of Cyclohexanone Formaldehyde Resin / Layered Silicate Nanocomposites, Poster Presentation, *Materials For Tomorrow Conference*, October 23-25 Göthenburg, Sweden.